



Review

Cartilage Integrity: A Review of Mechanical and Frictional Properties and Repair Approaches in Osteoarthritis

Przemysław Krakowski ^{1,2,*} , Adrian Rejniak ², Jakub Sobczyk ² and Robert Karpiński ^{3,4,*} 

- ¹ Department of Trauma Surgery and Emergency Medicine, Medical University, 20-059 Lublin, Poland
- ² Orthopaedic and Sports Traumatology Department, Carolina Medical Center, Pory 78, 02-757 Warsaw, Poland; adrian.rejniak@carolina.pl (A.R.); jakub.sobczyk@carolina.pl (J.S.)
- ³ Department of Machine Design and Mechatronics, Faculty of Mechanical Engineering, University of Technology, 20-618 Lublin, Poland
- ⁴ Department of Psychiatry, Psychotherapy and Early Intervention, Medical University, 20-059 Lublin, Poland
- * Correspondence: przemyslaw.krakowski84@gmail.com (P.K.); robert.karpinski@umlub.pl (R.K.)

Abstract: Osteoarthritis (OA) is one of the most common causes of disability around the globe, especially in aging populations. The main symptoms of OA are pain and loss of motion and function of the affected joint. Hyaline cartilage has limited ability for regeneration due to its avascularity, lack of nerve endings, and very slow metabolism. Total joint replacement (TJR) has to date been used as the treatment of end-stage disease. Various joint-sparing alternatives, including conservative and surgical treatment, have been proposed in the literature; however, no treatment to date has been fully successful in restoring hyaline cartilage. The mechanical and frictional properties of the cartilage are of paramount importance in terms of cartilage resistance to continuous loading. OA causes numerous changes in the macro- and microstructure of cartilage, affecting its mechanical properties. Increased friction and reduced load-bearing capability of the cartilage accelerate further degradation of tissue by exerting increased loads on the healthy surrounding tissues. Cartilage repair techniques aim to restore function and reduce pain in the affected joint. Numerous studies have investigated the biological aspects of OA progression and cartilage repair techniques. However, the mechanical properties of cartilage repair techniques are of vital importance and must be addressed too. This review, therefore, addresses the mechanical and frictional properties of articular cartilage and its changes during OA, and it summarizes the mechanical outcomes of cartilage repair techniques.

Keywords: cartilage; osteoarthritis; cartilage friction; cartilage biomechanics; friction; wear



Citation: Krakowski, P.; Rejniak, A.; Sobczyk, J.; Karpiński, R. Cartilage Integrity: A Review of Mechanical and Frictional Properties and Repair Approaches in Osteoarthritis.

Healthcare **2024**, *12*, 1648. <https://doi.org/10.3390/healthcare12161648>

Academic Editor: Flaviu Moldovan

Received: 29 June 2024

Revised: 9 August 2024

Accepted: 14 August 2024

Published: 19 August 2024



Copyright: © 2024 by the authors. Licensee MDPI, Basel, Switzerland. This article is an open access article distributed under the terms and conditions of the Creative Commons Attribution (CC BY) license (<https://creativecommons.org/licenses/by/4.0/>).

1. Introduction

Osteoarthritis (OA) is one of the main causes of disability around the world, especially among the elderly population. Although OA is considered an age-related disease, studies have shown that osteoarthritic changes can be found in a younger population [1–3]. The global burden of disease report estimates that over 527 million people suffer from OA [4,5]. The development of OA can be triggered by many different factors, including obesity, sports, genetic factors, previous injuries, work environment or joint anatomy abnormalities [6–8]. Osteoarthritis is also an important socioeconomic problem. It is estimated that the costs of OA can reach up to 2.5% of the gross domestic product [9]. With the aging of the population, an increase in OA prevalence is expected [10]. Articular cartilage (AC), which is a highly specialized tissue producing smooth, painless, and almost frictionless movement, is most significantly affected during OA progression. Moreover, cartilage presents very limited repair capacity [11–14]. Once the cartilage structure is compromised, osteoarthritic degeneration begins, leading to joint failure and pain as an end result [11,15]. The inevitable degradation of cartilage starts from its superficial layer [16], which is also the most important layer in preserving tribological properties due to its collagen orientation and composition. The surface roughness of healthy articular cartilage ranges from 1 nm

to 150 nm, depending on the joint [17]. Interestingly, the surface roughness of total joint replacements typically range from 40 nm to 200 nm [18]. Increased friction during OA progression as well as loads exerted on cartilage induce secretion of proinflammatory cytokines such as IL-1, which further increases surface roughness and friction [19,20]. Modern orthopedics considers cartilage as the most important structure to be preserved and protected in diarthrodial joints in order to reduce OA progression. Various joint-sparing treatments have been proposed in the literature, from conservative [21–24] up to different surgical treatment options, including microfractures, load-shifting osteotomies, various scaffold options, as well as cartilage culture and implantation techniques [25–28]. Clinical outcomes of those procedures have been extensively studied by orthopedic surgeons and most commonly survivor time (time when total joint replacement is required) is one the most important outcome measures. Nevertheless, no strict protocol for cartilage repair and regeneration has been established to date. To better understand the nature of cartilage regeneration techniques, orthopedic surgeons should understand the biomechanical and tribological properties of cartilage and its repair techniques. This review summarizes the anatomy and mechanical properties of healthy cartilage, as well as cartilage repair techniques.

2. Healthy Cartilage—Anatomy, Mechanical Properties, Synovial Fluid

The cartilage is a viscoelastic type of connective tissue, originating during the embryonic phase of human development, prior to the onset of osteogenesis [29]. Its mean thickness was estimated at 1.4 mm. However, it is worth noting that the study was performed on an elderly population, in which cartilage loss is to be expected. A more recent study by Guo et al., who analyzed a total of 700 MRI results, has found that articular cartilage thickness ranges from 1.79 mm to 3.13 mm depending on location [30].

The primary role of articular cartilage is to create a smooth, lubricated overlay for low-friction articulation and to allow loads to be transmitted to the underlying subchondral bone. The unique material properties of cartilage allow it to withstand strong contact forces while dispersing the ensuing compressive stimulus to the subchondral bone underneath. Hyaline cartilage consists of chondrocytes and an extracellular matrix (ECM). Chondrocytes are cells that exhibit a high degree of specialization and metabolic activity, performing a distinct function in the processes of extracellular matrix creation, maintenance and repair. They are characterized by low apoptotic activity and an inability to divide [31].

Chondrocytes derive from mesenchymal stromal cells and comprise around 2% of the overall volume of the articular cartilage [32]. Chondrocytes rarely form intercellular connections for signal transduction and transmission. However, they respond to growth factors, mechanical stresses, piezoelectric forces, and hydrostatic pressures. Schätti et al. showed that bone marrow mesenchymal stromal cells show upregulation in chondrocyte-specific gene expression when biaxial loading is applied [33]. Chondrocytes also affected by compression frequency. Sah et al. [34] showed that cyclic loading with a frequency of 0.1 to 1 Hz stimulates collagen and proteoglycans synthesis, while, on the other hand, static loading was related to dose-dependent ECM degradation [35]. Unfortunately, chondrocytes have a limited mitotic capacity, which, in turn, decreases the intrinsic capacity of cartilage for healing after injury [36,37].

The biochemical composition of cartilage includes water, collagen, and proteoglycans [36]. Cartilage is a type of tissue that exhibits anisotropic and viscoelastic features, enabling it to withstand compressive, tensile, and shear forces. The compressive strength of tissue is attributed to the presence of water and proteoglycans. This phenomenon is attributed to negative electrostatic repulsion forces [36,38]. Under compression, negative charges of proteoglycans are pushed closer together and, as a result, the repulsive force increases, adding significantly to cartilage stiffness [36,39,40]. The resistance to tensile stresses is mostly conferred by collagen fibrils. This is based on the mesh structure of collagen fibrils interconnections [41] and its unique arrangement depending on the cartilage layer. Hyaluronic acid, lubricin, and matrix permeability play a crucial role in reducing friction on the joint surface. Decorin, a tiny leucine-rich proteoglycan, regulates the micromechanics

and mechanobiology of the cartilage pericellular matrix. In vivo, as chondrocytes reside in an aggrecan-rich, highly negatively charged osmotic environment, decorin regulates chondrocyte mechanotransduction primarily via controlling the integrity of aggrecan in the PCM [42].

The surface of cartilage is enveloped by a delicate layer known as lamina splendens [30,43]. This layer is composed of proteins and exhibits an acellular and non-fibrous nature. Its thickness varies in the range from a few hundred nanometers to one micrometer. The formation of lamina splendens has been postulated to occur through a gradual build-up of proteins originating from synovial fluid. It provides a low-friction interface for cartilage and plays a key role in responding to mechanical loads [44]. It is also the first cartilage layer to degrade during the progression of OA [45]. However, chondrocyte implantation, for instance, does not regenerate lamina splendens [46].

The superficial zone lies beneath lamina splendens. It accounts for 10–20% of the cartilage thickness. The collagen fibers in this zone have relatively small diameters (18 ± 5 nm) and are packed tightly, running parallel to the surface [47]. This particular architectural arrangement is well-suited for effective dispersing and mitigating the impact of substantial shear stresses [48]. The proteoglycan concentration within this layer is comparatively low, resulting in its higher permeability when compared to other layers of cartilage [49–51]. And what is most interesting, permeability rather than layer thickness is responsible for dynamic friction in contrast to start-up friction, which is dependent on the layer thickness [52]. The chondrocytes located in the superficial zone of cartilage are in control of the secretion of lubricating proteins such as superficial zone proteins (SZPs) [53] along with collagen I [54]. These proteins are exclusive to the superficial zone, absent in the other layers of the cartilage [55].

The middle zone, which comprises 40–60% of the cartilage thickness, is distinguished by a reduced cellular concentration together with the presence of spherical chondrocytes. Type II collagen is the predominant ECM component inside this region [56]. The structure is composed of arcades that are interconnected by small-scale fibers with random orientations [48,57]. The middle zone exhibits the most elevated concentration of proteoglycans compared to other zones [49–51]. The chondrocytes located in the middle layer demonstrate a substantial expression of collagen II and proteoglycans, including aggrecan [56].

The region referred to as the deep zone, along with the calcified zone, which comprises 20–50% of the cross-sectional length, exhibits a cellular and collagen fiber organization that is oriented perpendicular to the subchondral bone. While the concentration of proteoglycans may rise, the cellular density in the deep zone is significantly lower in contrast to the middle and superficial zones [50,51]. Chondrocytes in this layer demonstrate a reduced capacity for synthesizing and secreting collagen II [58]. Collagen X secretion can also be observed in the deep zone, where it contributes to structural integrity and shock absorbance [59].

The deep and calcified zones are separated by a narrow line known as the “tidemark”. The tidemark acts as a means of anchoring more pliable and vertically aligned collagen fibrils found in the innermost region of non-calcified articular cartilage. This anchoring mechanism is considered to help protect these fibrils from being disrupted or torn at their attachment point to the calcified zone [60].

The calcified zone is composed of hydroxyapatite, which serves as a barrier between the rigid bone and the pliable cartilage, reducing a mechanical gradient [61]. The layered architecture of cartilage is presented in Figure 1.

In addition to the presence of zone-related differences in the structure and composition of cartilage, the matrix is composed of numerous specified regions that are delineated by factors such as closeness to chondrocytes, composition, and collagen content. The ECM is divided into the pericellular, territorial, and interterritorial regions [36], as shown in Figure 2. In this context, it can be observed that each chondrocyte is enveloped by a translucent pericellular glycoalyx matrix (Pg) and is also enclosed by a pericellular capsule (Pc). This structure is known as the chondron [62]. A combination of these two constituents

is commonly known as the pericellular matrix. The pericellular capsule is enveloped by a territorial matrix (Tm) and an interterritorial matrix (Im), which is sometimes referred to as ECM [63]. A notable presence of aggrecan, link protein, and hyaluronan can be observed inside a pericellular matrix (Pg and Pc) [64]. It can, however, be noticed that these macromolecules are in a dissociated state and that the aggrecan–hyaluronan complex has not yet been formed. The collagen composition exhibits variations in comparison to the bulk or interterritorial matrix (Im) of cartilage [65]. Collagen II is observed in the form of slender strands, with their diameters ranging from 10 to 15 nanometers, which are intricately intertwined to create a compact and densely woven arrangement known as the pericellular capsule [64]. This architectural structure is believed to function as a hydrodynamic mechanism for safeguarding chondrocytes during loading. It acts as a pliable cushion that is capable of supporting load by reversible deformation depending on the amount of stress [66]. According to Chandrasekaran et al., SEM scans revealed intricate collagen fibril structures on the mandibular condyle cartilage and articular disk. The fibrillar diameter on the condyle cartilage surface was 22.3 ± 0.3 nm (mean \pm 95% CI from 300 fibrils measured on $n = 3$ animals), significantly thinner ($p < 0.0001$) than those on the disk surfaces (33.4 ± 0.4 for superior surface, 32.9 ± 0.5 for inferior surface, both statistically comparable). Additionally, differences in fibril sizes were observed on the disk surfaces. The anterior end had the thickest fibrils (35.6 ± 1.1 nm), while the medial region had the thinnest (31.3 ± 0.8 nm). On the inferior side, the front end similarly had the thickest fibrils (34.0 ± 1.0 nm), and the central region had the thinnest (31.2 ± 0.9 nm) [67]. Collagen types IX and VI, along with collagen II, present increased quantities within the pericellular matrix, as opposed to the interterritorial matrix [62]. As previously elucidated, these collagens actively engage in cross-linking processes to contribute to the development of more substantial collagen II bundles. The composition of the territorial matrix (Tm) closely resembles that of the interterritorial matrix, except for the thinner collagen II fibrils and a larger assembly of proteoglycans, particularly chondroitin sulfate [68].

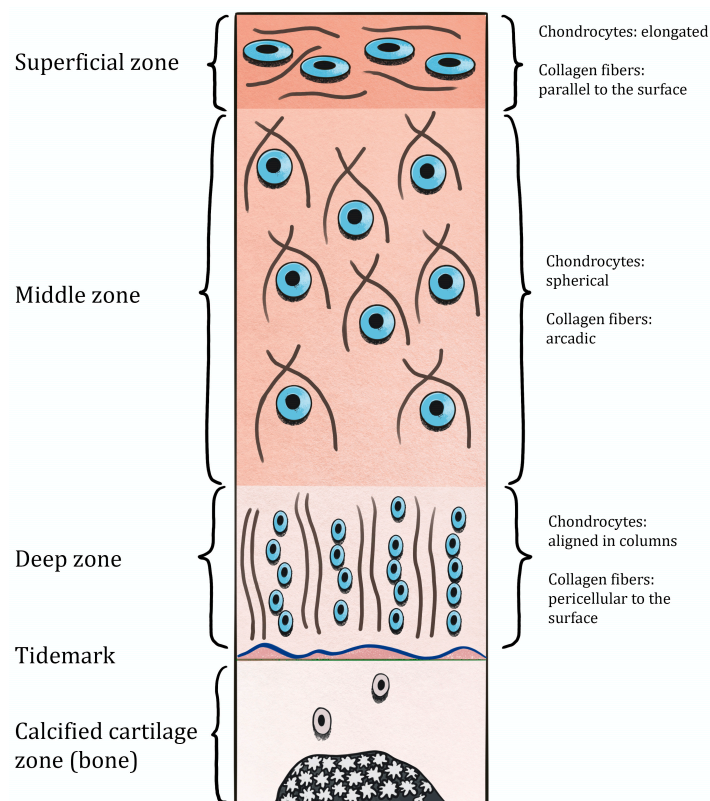


Figure 1. Cartilage layers illustrating differences in collagen mesh structure and chondrocyte arrangement.

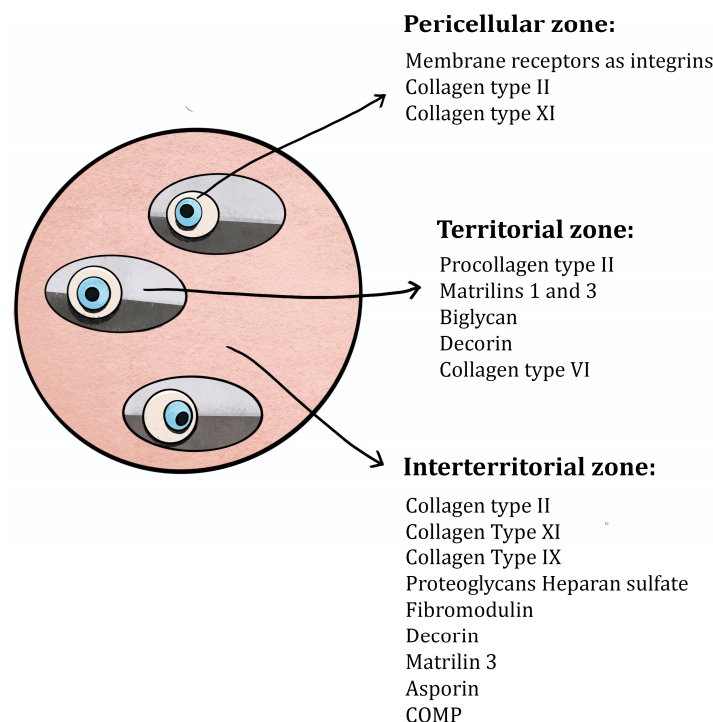


Figure 2. Cross-sectional view of ECM, with a division into pericellular, territorial, and interterritorial cartilage sections.

Collagen (75% of the dry weight) and proteoglycan (20–30% of the dry weight) are the primary load-carrying structural segments of the extracellular matrix, and their concentrations and architectures vary depending on the depth from the articular surface [69,70]. The following collagen types can be found in the hyaline cartilage: III (10%), IX (1%), XI (3%), as well as VI (1%, solely in the pericellular matrix surrounding chondrocytes) [71]. The surface zone has the maximum collagen concentration, with a 20% decrease in its concentration in the middle and deep zones. The content of proteoglycans is the lowest in the superficial zone and increases by up to 50% in the middle and deep zones [69,70]. The superior resistance to shear forces of the superficial zone among the four zones can be linked to the unique organization of collagen fibrils [72–74]. Moreover, the superficial zone protein, which is only produced by chondrocytes located in the superficial layer, further decreases friction and, therefore, protects cartilage against shear forces [75]. This is now recognized to be the very same molecule as the megakaryocyte-stimulating factor or lubricin [76]. Furthermore, it is synthesized by synovial cells. The concept is that lubricin plays a predominant role in supplying the almost frictionless articulation provided by the articular cartilage [76]. Collagen exhibits a limited elongation of less than 10% of its overall length, with a significant portion of this elongation attributed to the straightening of the fibers rather than to actual extension [77]. When all collagen molecules reach a straight configuration oriented perpendicular to the pulling axis and the entire potential for molecular straightening is used up, the collagen molecules themselves stretch, resulting in a markedly increased tangent microfibril stiffness at strains greater than 10% [78].

The articular cartilage is composed of two distinct phases: fluid and solid. The articular cartilage is primarily water, which constitutes up to 80% of its wet weight. About 30% of the water is located in the intrafibrillar region within the collagen structure, whereas a little proportion is located within the intracellular area. The residual fraction is confined to the interstitial voids of the matrix [79,80]. The tissue water contains dissolved inorganic ions, including sodium, calcium, chloride, and potassium [81]. The water concentration exhibits a gradual decrease from approximately 80% in the surface zone to 65% in the deep zone [82]. Its movement within cartilage and over the articular surface facilitates the transportation and dispersion of nutrients to chondrocytes, while also serving as a

lubricant [36]. The interaction of proteoglycan aggregates and interstitial fluid results in negative electrostatic repulsion forces, providing articular cartilage with compressive resilience [36]. An instant application of articular contact forces during joint loading results in a rise in the interstitial fluid pressure. This causes the fluid to leak out of the ECM, creating a significant frictional drag on the matrix [83,84]. When the compressive force is released, the interstitial fluid returns to cartilage. The fluid cannot be easily squeezed out of the matrix due to the limited permeability of the articular cartilage [85]. The two opposing bones, along with the surrounding cartilage, serve to enclose and restrict the movement of the cartilage located beneath the contact surface. The purpose of these boundaries is to limit or control mechanical deformation.

Since the articular cartilage is naturally avascular, synovial fluid (SF) is an essential component of the biomechanical behavior, lubrication, and metabolism/nutrition of this tissue. The composition of SF, which is a dynamic reservoir of proteins produced from synovial and cartilage tissue, may serve as a biomarker for the health and pathophysiologic state of the joint. It has a consistency which can be compared to an egg white. Hyaluronic acid, lubricin (a protein from the superficial zone), and phospholipids at physiological amounts work in concert to enable SF to act as a boundary lubricant and reduce border friction in cartilage [86,87].

Glycosaminoglycans (GAGs), proteoglycans, and glycoproteins are some of the non-collagenous components of the ECM ground substance that are connected to the fibrillar components. GAGs are sugars composed of repeating disaccharide units that give rise to six primary subunits of articular cartilage: chondroitin sulfates 4 and 6, keratin sulfates, dermatan sulfate, heparan sulfate, and hyaluronan (or hyaluronic acid) [88]. They are negatively charged, repelling one another while drawing ions (such as Ca¹¹ and Na¹) and water to them. This ensures that their primary functional characteristics, i.e., water absorption and maintenance of the mechanical properties as well as ECM hydration, are maintained [77,89].

3. Factors Affecting the Mechanical Properties of Cartilage

The articular cartilage is responsible for load-bearing as well as facilitating translational and rotational movements inside the adjacent joint [90]. The biphasic composite material of articular cartilage is characterized by an intricate structure and composition, which allows it to effectively trap liquids while maintaining its fibrous and porous nature [91]. When an external force is exerted on the system such as the application of a load, the synovial fluid confined inside the system becomes pressurized. As a result, the pressurized synovial fluid squeezes through the surrounding tissue, developing frictional resistance against the solid matrix. This frictional drag facilitates the transfer of the applied load within the system [92]. The exceptional load-bearing properties of articular cartilage can primarily be attributed to load-transmission and fluid-pressurization mechanisms [93–95]. The material's biphasic and viscoelastic characteristics have significant implications for its reaction to compressive, tensile, and shear loads. These responses are unevenly distributed across the depth of the mature cartilage [96]. Multiple evaluation methods have been implemented to study the mechanical properties of cartilage. The methods are described at the end of this Section.

3.1. Compressive Strength

The permeability and viscoelasticity combination is thought to be responsible for the compressive characteristics of cartilage. Due to its inherent traits, articular cartilage exhibits a non-linear reaction when subjected to mechanical forces, owing to its inhomogeneity, anisotropy, and poro-viscoelastic nature. The tissue has poor permeability, resulting in rapid pressurization of the interstitial fluid. The tissue's hydraulic permeability and aggregate equilibrium compression modulus significantly depend on the water content and uronic acid concentration. This relationship serves as a physicochemical foundation for the observed reduction in the tissue's permeability as compression increases [97–100]. The movement of interstitial water via the ECM leads to certain time-dependent reactions in the

articular cartilage [101]. Tissue creep may require around 1000 s of load application to attain a condition of new equilibrium [101] and additional time for stress relaxation to achieve a state of equilibrium. It is worth mentioning that an increase in ECM deformation leads to a decrease in the average size of pores. Consequently, this results in an increased diffusional resistance between the interstitial water and the ECM [102]. The duration required to attain the equilibrium condition depends on the magnitude of load or displacement.

When an external force is applied, the fluid that was previously constrained within the tissue starts to move. Due to poor permeability of cartilage, this results in pressurization and generation of significant drag forces on the solid phase. These drag forces help to dissipate the stress [103]. When cartilage undergoes deformation, there is a drop in its porosity, resulting in reduced permeability. The values of permeability in cartilage normally fall within the range of 0.1 to $10 \times 10^{15} \text{ m}^2/\text{Pa s}$ [94]. This means that the cartilage responds to external loads through the augmentation of hydraulic pressure and mechanical rigidity [99]. Joint cartilage compressive forces exhibit a fleeting nature in spite of their considerable magnitudes. These forces escalate from around 1–2 atmospheres during unloading [104] to a range of 100–200 atmospheres when an individual assumes an upright position. Furthermore, these forces cyclically fluctuate between 40 and 50 atmospheres [105]. The explanation for the compressive properties of cartilage has been traditionally grounded in the biphasic theory. This study identifies three primary forces: (a) a stress exerted by the solid phase, which is presumed to adhere to Hooke's law and exhibit a linear stress–strain behavior; (b) a pressure generated by compression of the liquid phase, which, as previously mentioned, exhibits a time-dependent behavior; and (c) a friction generated between the liquid and solid phases. The fluid phase generates friction, which may be characterized using a linear formulation of Darcy's law [106]. This friction depends on the permeability of the tissue and the pressure generated, both of which vary with time. Upon removal of the load, the tissue undergoes a process of regaining its initial shape. This recovery is facilitated by two mechanisms: the Donnan osmotic pressure effect [107], which redistributes the fluid inside the compressed region, and the presence of elastic qualities inherent in the solid phase [55]. The variability of the compressive characteristics is associated with the disparity in fluid flow. Consequently, the superficial zone, which exhibits a high level of permeability, is subjected to compressive forces reaching a maximum of 50%. The fluid flow experiences a significant reduction in the medium and deep zones, leading to compressive strains that are below 5% [108]. Cartilage deformation is prevented through its low permeability, which results in fluid pressurization, and the impermeability of the subchondral bone, which provides stability to the tissue. Throughout the course of the day, there are repeated instances of compression-relaxation events, resulting in strains of which 15–20% are irreversible. The original shape can be fully restored only after extended periods of rest [109].

3.2. Tensile and Shear Properties of Cartilage

The tensile and shear properties of cartilage can be observed when subjecting it to a compressive force. Deformation manifests itself as the generation of tensile tension on the surface. The force in question is tangential in nature, acting parallel to the surface. It is sustained by the solid phase which is composed of collagens and proteoglycans. In addition, the generated tension is responsible for inducing a viscoelastic reaction, which arises from the displacement of collagen fibers. In the initial stages, the generation of tension in the superficial zone results in the amplification of modest stresses into significant strains. This phenomenon can be attributed to high permeability of the region, which facilitates a quick outflow of the fluid. The need for greater levels of stress to achieve equivalent strain is a consequence of the friction induced by the movement of collagen networks through proteoglycans [32,36]. During the concluding phase, the collagen fibers undergo stretching and assume the responsibility for withstanding the entirety of the externally exerted force, hence leading to the manifestation of an elastic reaction. The articular cartilage experiences shear pressures as a result of the translational and rotational

motion of bones. Its primary support comes from the solid phase of the tissue. Empirical investigations have been conducted to determine the equilibrium shear modulus, finding it to range from 0.05 to 0.25 MPa. The values of the dynamic shear modulus and the loss angle have been determined to range from 0.1 to 4 MPa and approximately 10 degrees, respectively [110,111].

At the macroscale, the mechanical qualities of cartilage depend on the cell shape and distribution from the superficial to deep cartilage, the orientation of collagen fibers, and the amount of proteoglycans. Huttu et al. [112] reported notable positive associations between the elastic modulus and both proteoglycan levels and collagen content in their analysis of the total thickness of cartilage samples. However, when focusing solely on superficial cartilage which constituted approximately 20% of the total thickness, positive correlations were observed but they did not reach statistical importance. Similar correlations were documented in a prior investigation by Nissinen et al. [113], who studied the proteoglycan concentration and the modulus of the fibril network. These correlations were observed at both 30% and 50% of the total depth. Furthermore, Ilnatouski M. et al. [114] established a correlation between the elastic modulus and the indentation depth (h) measured by atomic force microscopy (AFM). The elastic modulus exhibited a peak value of 1.7 MPa, which decreased to 0.5 MPa as the indentation depth was increased from 25 to 150 nm. In contrast, Fischenich et al. [115] discovered that the average modulus exhibited an upward trend as the depth on human condyles increased, whereas the permeability was reduced. However, in addition to examining the superficial zone, Fischenich et al. [115] also conducted tests at a depth of 500 μm beneath the articular surface and 500 μm above the calcified cartilage. Important relationships were observed between the mechanical behavior and the collagen orientation or biochemical makeup with respect to fiber orientation and depth. Significant correlations were established between the mechanical properties of moduli and their chemical composition, as well as between the permeability coefficient and the orientation of collagen.

3.3. Tribological Properties of Cartilage

Previous studies [103,116,117] have shown that, in contrast to other mechanical features, tribological properties do not depend on the location. However, it is worth noting that the presence of OA has a significant impact on these properties. A study conducted by Moore et al. [117] revealed distinct tribological characteristics resulting from osteoarthritis (OA). The researchers observed an escalation in shear stresses originating from the superficial zone and propagating towards the deep zone. This phenomenon led to the deterioration of the layers across the entire thickness, ultimately culminating in a slow loss of the material.

A gradual transmission of the applied stress from the fluid medium to the pliable cartilage tissue is a consequence of the fluid's involvement inside the solid matrix, ultimately leading to the attainment of an equilibrium state. The friction coefficient of articular cartilage has been demonstrated to fluctuate throughout a wide range (from 0.002 to 0.5) depending on the loading arrangement [118,119]. The maintenance of a low friction coefficient within a certain range [116] depends on the presence of interstitial fluid that effectively lubricates the cartilage surfaces. The process of transitioning from dynamic loading to static loading results in reduced energy dissipation, which is effectively compensated by the presence of interstitial fluid that seeps into cartilage. The absorption of synovial fluids by the cartilage components is responsible for initiating the boundary lubrication process, primarily due to low velocities and the quasi-static environment involved. The process of aging or the presence of joint illness results in decreased glycosaminoglycan levels, hence leading to an elevation in the rate of coefficient of friction [120]. Kienle et al. [121] conducted an investigation into the impact of lubricating fluid on the friction and wear characteristics of the ovine articular cartilage in both boundary and mixed lubrication regime. Four different lubricants were investigated in the study: ddH₂O, 154 mM NaCl solution (representing physiological concentration), 2 M NaCl solution, and synovial fluid.

An increase in the coefficient of friction was observed via atomic force microscopy (AFM) when the salt concentration was increased at the microscale. However, opposite results were obtained from macro-friction experiments conducted at sliding speeds greater than 0.1 mm/s. This discrepancy could be attributed to an ionic repulsion between the experimental setup and the cartilage, which resulted in a lower measured friction force. In their study, Hossain et al. [122] observed that the coefficient of friction (COF) in bovine cartilage samples did not exhibit any anisotropy when subjected to a normal load applied parallel or perpendicular to the direction of collagen fibers on the superficial layer of cartilage. This lack of anisotropy was observed despite the presence of glycosaminoglycan loss and collagen damage that extended throughout the depth of the cartilage tissue, particularly for the cases of wear in the transverse direction. Moreover, few studies have focused on the frictional characteristics of human cartilage. In a study by Middendorf et al. [123], the coefficient of friction between human cartilage and glass was assessed using a specially designed pin-on-plate apparatus. The study reported the average coefficient of friction to be in the range of 0.22 ± 0.016 . In a similar vein, Li et al. [124,125] investigated the frictional characteristics of AC via pin-on-plate friction tests, with contact made against various surfaces including cartilage, stainless steel, and polyvinyl alcohol (PVA). The coefficient of friction values obtained from the cyclic tests were found to be 0.029, 0.159, and 0.076 for the interactions of cartilage-on-cartilage, cartilage-on-stainless steel, and cartilage-on-PVA, respectively. A summary of the articular cartilage mechanical properties is given in Table 1, according to Little et al. [126].

Table 1. Experiments into the mechanical properties of articular cartilage.

Author	Mechanical Property	Value	Mechanical Tests
Mow VC et al. [94]	Aggregate modulus (MPa)	0.1–2.0	Confined compression, indentation
Mow VC et al. [94]	Hydraulic permeability (m^4/Ns)	10^{-16} – 10^{-15}	Confined compression, Unconfined compression, Indentation
Mow VC et al. [94]	Compressive Young's modulus (MPa)	0.24–0.85	Unconfined compression
Little et al. [126]	Poisson's ratio	0.06–0.3	Unconfined compression, Indentation
Little et al. [126]	Tensile equilibrium modulus (MPa)	5–12	Tensile stress relaxation
Ihnatouski et al. [114]	Tensile Young's modulus (MPa)—constant-strain rate	5–25	Tensile constant strain rate
Little et al. [126]	Tensile strength (MPa)	0.8–25	Tensile constant strain rate
Wenbo Zhu et al. [110]	Equilibrium shear modulus (MPa)	0.05–0.4	Equilibrium shear
Wenbo Zhu et al. [110]	Complex shear modulus (MPa)	0.2–2.5	Dynamic shear
Wong et al. [111]	Shear loss angle (\circ)	10–15	Dynamic shear
McCutchen CW et al. Forster H et al. [118,119]	Friction coefficient	0.002–0.5	

Cartilage also presents thixotropic properties which are time-dependent shear-thinning properties. Articular cartilage exhibits thixotropic properties, meaning its viscosity changes under the influence of load and shear, then returns to its original state once these

forces are removed. This allows the cartilage to adapt to varying mechanical conditions within the joint. Under load, the viscosity decreases, facilitating movement and cushioning; while, at rest, it returns to its initial level, ensuring joint stability [127–129]. Thixotropy protects the joint from excessive friction and wear, while also enabling smooth and safe movements. Over the time of using the knee joint, the viscous properties of SF change and become less resistant to shear forces [130].

As shown above, the mechanical properties of cartilage differ depending on the evaluation method. Below, we summarize the testing protocols mentioned in our review to give a clear insight into the differences between the evaluation methods.

(a) Atomic Force Microscopy

Atomic Force Microscopy (AFM) is a nanostructural imaging technique that uses submicron resolution to investigate sample surfaces (e.g., cartilage) [114,131]. A simple AFM setup for biomechanical applications involves a silicon pyramidal probe (radius tip of around units-tens of microns) [114] or a polystyrene or borosilicate glass sphere [121,132] positioned on a flexible cantilever fixed to an electrical piezo. During the approach phase, Van Der Waals forces interact with the sample surface. The attraction forces cause the cantilever to deflect towards the sample surface. The cantilever deflection changes the direction of the laser beam reflected from the backside of the cantilever, allowing for a very accurate deflection measurement through optical beam detection. AFM can also be used to examine specific structures like cytoskeleton and detect dynamic changes in submembranous structures [133]. By applying a continuous load to the cantilever tip and measuring the surface lateral force [132], AFM may also be utilized to study the tribological characteristics of the cartilage in the boundary-lubricated regime [121]. Since AFM can only be used to investigate a limited scanning region [114], large-scale measurements can be performed with a rotational macrotribometer (e.g., a rheometer fitted with a tribology measuring cell) [121].

(b) Indentation test

A quantification of tissue/cell stiffness in terms of instantaneous modulus (IM) or equilibrium modulus (E_{eq}) is acquired from indentation testing, and due to material heterogeneity, the results may differ from one point to another because only sections of the total samples are analyzed. Colored maps can be used to emphasize the variety in tissue mechanical characteristics within the same sample [134,135] as well as tissue degradation caused by diseases such as OA. Plane-ended or spherical-tipped indenters are applicable depending on the required stiffness qualities and sample thickness. When assessing cartilage stiffness on small joint surfaces, indentation testing may be recommended because obtaining regular samples for mechanical testing might be difficult and damaging to the tissue [136].

(c) Compression test

Articular cartilage comprises both a solid and a fluid phase, thus compression tests are classified as either confined [137] or unconfined [138]. The setup and outcomes vary depending on the employed test method. Confined compression is typically accomplished by placing a cylindrical disk of the testing material within a limited impermeable chamber with one porous plate [137]. The sample and the porous plate are then subjected to an axial fluid flow caused by a compressive force operating perpendicular to the plate. After a relaxation time (Zimmerman et al. [137] reported roughly 1 h of relaxation time to see the equilibrium stress plateau), this test allows direct measurement of solid matrix stiffness (aggregate modulus, HA) and material permeability (K). Unconfined compression, on the other hand, entails placing the sample between two impermeable plates and squeezing the plates together at a specific velocity, causing the fluid to leak from the material and the sample to deform radially [139]. After applying a constant displacement until equilibrium is established, this test is often employed to achieve both instantaneous (instantaneous modulus) and long-term properties, i.e., E_{eq} . Relaxation periods differ, ranging from

15 min [140] to 2 h [138] depending on the imposed strain amplitude (from 5% to 25%, respectively). In stress-relaxation experiments in unconfined compression with plane-ended indentation, loading regimens with 4 to 6 ramps of increasing strain amplitude of 3–5% have been widely used.

(d) Tensile test

Tensile tests must be performed using an uncommon setup in order to keep the samples hydrated in a saline solution throughout the course of testing. Rectangular sheet-like samples are collected from the AC and then attached to the machine grips at both ends in order to apply imposed displacement and measure force. Tensile tests are used to characterize fracture strength [141] or step-wise stress-relaxation testing [139,142] to discover immediate and equilibrium parameters. In comparison to other tests, tensile tests on human cartilage yielded lower velocities (0.08 mm/s) and strain rates (0.2%/s)

(e) Friction Test

The AC should also provide a frictionless surface during joint action to avoid high stress concentration and subsequent wear and erosion of the cartilage. In general, the frictional properties of two surfaces in contact, i.e., the associated coefficient of friction (COF), are affected by a variety of factors, including surface characteristics, roughness, and anisotropy [133,134], as well as the friction-regime-defining sliding (dry or lubricated) friction [143–145]. In the case of the AC, the COF may depend on the test type (i.e., rotating [146] or sliding [147,148]), cartilage source (e.g., both species and site), test speed and length, as well as ECM subcomponents such as the GAG content [146,149]. Furthermore, depending on the experimental setup design, different friction regimes, i.e., boundary vs. mixed lubrication, are measured. Friction tests performed on cut samples (e.g., cartilage plugs with a pin on plate arrangement) [148,149] have shown that the time to achieve the equilibrium COF linearly increases with the cartilage plug area, due to a strong influence of interstitial fluid pressurization on the COF of cartilage [92]. Maintaining a stationary contact area during the test (for example, ensuring that cartilage cylindrical plugs glide against an impermeable surface like that of metal) [149] results in a virtually stationary normal pressure. As a result, the COF is initially low and gradually rises as the load is shifted from the fluid to the solid matrix [92,149]. When a convex body slides across the cartilage surface, a migrating contact area is formed, resulting in the migration of the contact pressure field during sliding. This state reflects the natural circumstances within joints, with an almost constant low COF and interstitial fluid pressure (assuming that the fluid flow rate within the tissue is slower than the sliding velocity) [92,150,151]. In an unconfined compression test [146], compressive forces, torque, displacement, and rotational data were measured to calculate the torsional coefficient, while a pin-on-plate machine was built to perform sliding tests of cartilage vs. cartilage with PBS as lubricant [148] in order to obtain both the static and dynamic sliding COF.

4. Mechanical and Tribological Changes Induced by Osteoarthritis

Osteoarthritis (OA) is a complex disorder that exhibits diverse clinical manifestations depending on its specific anatomical sites, natural progression, clinical subtypes, and different etiological variables. The articular cartilage within a healthy joint has the capacity to endure substantial forces that arise from weight-bearing and joint movement throughout an individual's lifespan. A hypothesis was formulated that persistent excessive stress and compromised biomechanical factors had detrimental effects on the joint, ultimately leading to the degradation of articular cartilage and a subsequent inflammatory response. Consequently, these symptoms later resulted in stiffness, edema, and reduced mobility. The current understanding is that osteoarthritis is a multifaceted process involving several inflammatory and metabolic variables [152,153].

4.1. Molecular Changes

During the early phases of osteoarthritis (OA), chondrocytes exhibit limited capacity for effective restoration of the damaged matrix. This is mostly due to an increasing activity of catabolic cytokines and matrix-degrading enzymes which hinder the repair process [154]. Unfortunately, this initiates the release of proteoglycans and the degradation of type II collagen on the cartilage surface. Subsequently, an elevation in water levels occurs, which is linked to the depletion of negatively charged glycosaminoglycans. This depletion subsequently leads to matrix swelling [155–157].

The breakdown of the cartilage matrix begins in the surface zone of cartilage and then expands into further zones as OA advances [158]. This phenomenon is correlated with a significant decline in the tensile strength of the extracellular matrix [159]. The breakdown of collagen and proteoglycan molecules, which are subsequently internalized by synovial macrophages, elicits the secretion of proinflammatory cytokines such as $\text{TNF}\alpha$, IL-1, and IL-6. The binding of these cytokines to the receptors on chondrocytes results in a subsequent release of metalloproteinases and a suppression of type II collagen synthesis, thereby promoting the breakdown of cartilage [160]. IL-1 β is considered a fundamental cytokine for OA progression. This cytokine not only induces secretion of proteases but also inhibits key type II collagen synthesis by osteoblasts [161]. This mechanism is supported by $\text{TNF-}\alpha$ [162] and IL-6 [160].

Alterations in PCM micromechanobiology are among the earliest signs of OA onset. Aggravated chondrocyte catabolism causes local degradation of proteoglycans, particularly aggrecan, in the PCM, resulting in worse micromechanical characteristics. This disrupts chondrocytes' normal mechanosensing, contributing to the vicious cycle of cartilage breakdown in OA. The local PCM micromodulus (Eind, PCM) and mechanically induced chondrocyte $[\text{Ca}^{2+}]_i$ activity are two crucial early indications of PTOA onset. Attenuating PCM degradation can protect chondrocyte mechanosensing, potentially protecting joint health, as local alterations occur before larger matrix changes. Exploring cell-ECM mechano-crosstalk at the nm-to- μm scale provides a basis for creating novel ways for early PTOA identification or treatments by targeting cartilage PCM [163]. These findings may also have implications for other load-bearing illnesses.

Multiple proteases have been described as OA triggers in the literature, out of which the most important are MMP-1, -3, -9, and 13 [164]. What is worth noting is the fact that degraded ECM components are a stimuli for further inflammatory response, which, as a result, progresses the OA. Antibodies directed against ECM proteins can be found in serum samples from patients with osteoarthritis and rheumatoid arthritis [165,166].

Apart from cartilage degradation and inflammatory activation, gross remodeling of subchondral bone is also present and proposed as a trigger towards further cartilage degradation [167]. Platelet-derived growth factor (PDGF) elevated levels in subchondral bone promote vessel formation and, therefore, progression of OA [168]. Another cytokine secreted by osteoblasts in subchondral bones is prostaglandin E2 [169], which has a detrimental effect on cartilage mostly by increasing the production of MMPs.

4.2. Structural Changes

At the macroscopic level, alterations in the composition of the cartilage matrix coincide with the emergence of surface fibrillations, which are characterized by the presence of microscopic cracks in the superficial zone. As OA advances, these cracks contribute to the detachment of cartilage fragments and the development of fissures that expand into the deeper layers of cartilage. Subsequently, the deep fissures within the affected cartilage cause its delamination, exposing the underlying zones of the calcified cartilage and subchondral bone [170–172]. Figures 3–6 show the course of cartilage loss in a knee joint according to the ICRS [173] grading system. These changes include an increase in the volume, thickness, and outline of the cortical plate, as well as changes in bone mineralization and material characteristics. Additionally, OA is associated with changes in the architecture and mass of the subchondral trabecular bone, the development of bone

cysts, and the presence of bone marrow lesions and osteophytes [174–176]. Subchondral bone cysts are frequently observed in individuals with advanced osteoarthritis. A concept has been developed that cysts are created within the subchondral bone, specifically at places where previous bone marrow lesions are present. This observation suggests that the development of cysts is directly linked to bone damage and necrosis, which, in turn, triggers the process of osteoclast-mediated bone resorption, ultimately resulting in cyst formation [177]. Osteophytes may potentially play a role in joint stabilization rather than actively contribute to the advancement of joint disease. Certainly, the elimination of osteophytes has been seen to result in increased joint instability in animal models of osteoarthritis [178]. Moreover, it is worth noting that no discernible correlation exists between the advancement of knee OA and the dimensions of osteophytes in human individuals with OA [179].

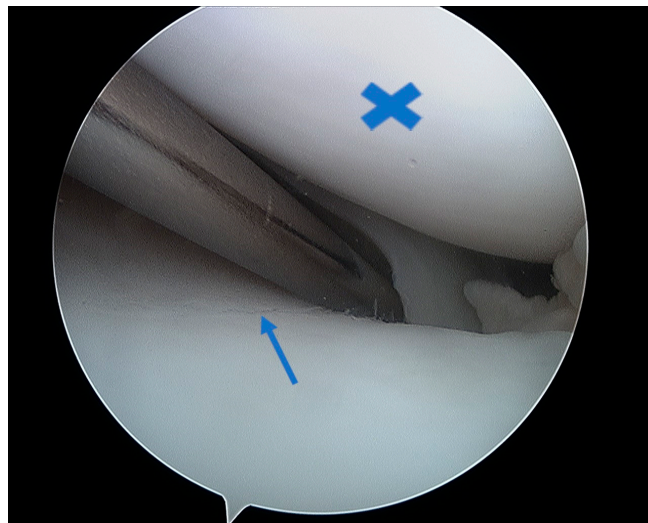


Figure 3. Arthroscopic view of healthy cartilage on the medial femoral condyle (asterisk) and grade I lesion on the medial tibial condyle with visible superficial layer fibrillation (arrow).

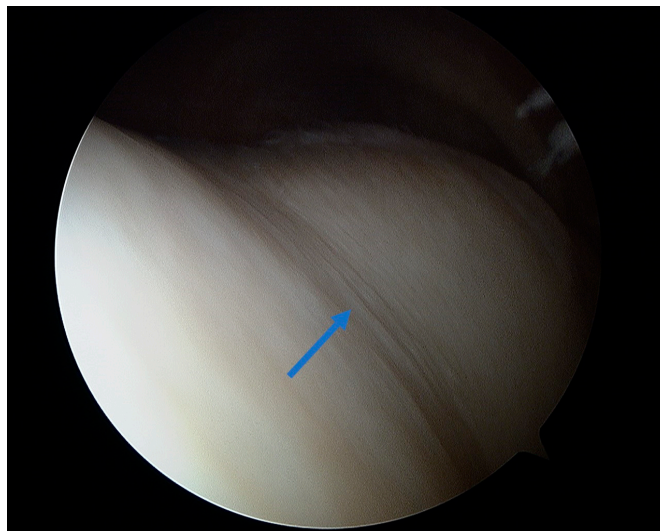


Figure 4. Arthroscopic view of grade II lesion on the femoral trochlear groove with visible longitudinal fissures (arrow).

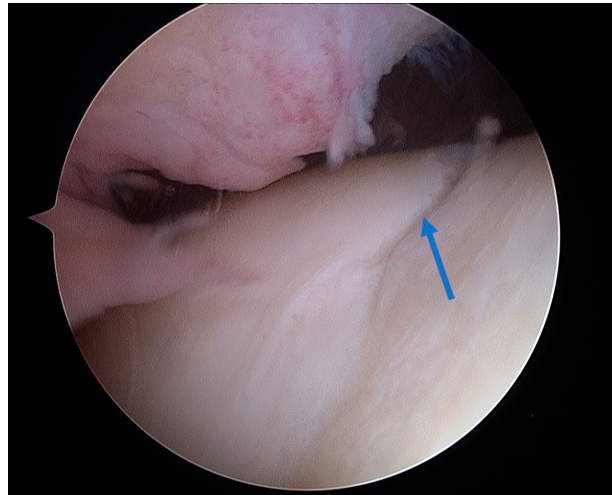


Figure 5. Arthroscopic view of grade III lesion with a visible cartilage deficit of less than 50% (arrow) in the femoral trochlear groove.

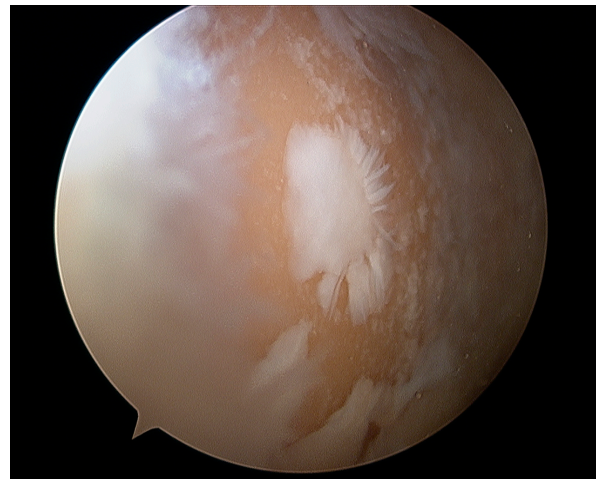


Figure 6. Arthroscopic view of grade IV lesion with subchondral bone exposure and complete cartilage loss, with only islands of cartilage visible on the medial femoral condyle.

4.3. Synovial Fluid Changes

The synovium is a distinct type of connective tissue that serves as a lining for diarthrodial joints, envelops tendons, and constitutes the inner layer of bursae and fat pads. The synovium plays a crucial role in regulating the quantity and content of synovial fluid (SF), primarily through the synthesis of lubricin and hyaluronic acid. The synovium plays an important role in facilitating chondrocyte nourishment, together with the subchondral bone. This is particularly important because articular cartilage lacks its own vascular or lymphatic supply [180].

The synthesis and secretion of proteoglycan 4 (PRG4) protein, also known as lubricin, occur within articular joints, specifically articular chondrocytes [181] and synoviocytes [182] in the superficial zone. Lubricin is detected inside synovial fluid [183] and is also found at the surface of articular cartilage. Lubricin functions as a boundary lubricant, facilitating the reduction in friction during contact between the cartilage surfaces. In this context, lubrication is achieved through molecular interactions occurring at the surface. Additionally, it exhibits a synergistic effect with hyaluronan (HA) to further diminish friction to a level that is almost equal to that of complete synovial fluid [86]. HA levels are diminished in osteoarthritis compared to the healthy joint [184]. Similarly, subsets of people with OA exhibit a diminished lubricating capacity in relation to lubricin [185]. Kosinska et al. [186] quantified the levels of HA and lubricin in synovial fluid samples obtained from healthy

joints, as well as from joints at different stages of osteoarthritis, including early-stage (eOA) and late-stage (IOA) osteoarthritis. The concentrations of HA were found to be the highest in the control SF, with a mean value of 2.2 mg/mL (range: 1.6–3.7 mg/mL). In comparison, the levels of HA in eOA SF were significantly lower, with a mean value of 1.7 mg/mL (range: 1.1–1.9 mg/mL). Similarly, the accumulation of HA in IOA SF were also lower, with a mean value of 1.9 mg/mL (range: 1.5–2.3 mg/mL), although this difference was not statistically significant. The levels of HA in eOA SF were 23.7% lower than those in the control SF, while the levels in IOA SF were 14.0% lower. The amount of lubricin in the control synovial fluid was measured to be 364.4 µg/mL (305.0–404.8 µg/mL). This concentration was found to be 1.5 times higher compared to the concentration of lubricin in the synovial fluid of individuals with early osteoarthritis (eOA), which was measured to be 244.5 µg/mL (119.6–381.7 µg/mL). Significantly, compared to the control synovial fluid, the content of lubricin in the synovial fluid for individuals with osteoarthritis decreased by 58.2% [152.3 µg/mL (108.2–183.9 µg/mL), $p = 0.005$]. The facilitation of low friction in the boundary mode and its potential impact on the shear deformation of cartilage is attributed to the lubrication of articular cartilage by synovial fluid. When conducting experiments on articular cartilage, researchers have observed that the presence of synovial fluid and its lubricant molecules can lead to reduced friction on the articular surface, thus demonstrating the effects of boundary lubrication [86,187]. The substitution of SF lubrication with phosphate-buffered saline (PBS) leads to an increase in boundary-mode friction [187].

Prior research has demonstrated that synovial fluid derived from human joints afflicted with OA exhibits typical lubricating properties [188]. Conversely, a reduction in the lubricating capacity of synovial fluid has been documented following several inflammatory and traumatic events, such as rheumatoid arthritis, [189] knee joint effusion after trauma, [188] meniscus removal, [190], and anterior cruciate ligament disruption [191]. A correlation has been discovered between a decrease in lubricin levels and an increase in friction inside the whole joint [108,189,191]. Teeple et al. [192] observed a marked decrease in the overall joint lubrication and an accompanying rise in friction persisting beyond the initial acute phase of the injury. The specific mechanisms underlying the deficit of lubricin remain unclear, although potential factors include reduced expression of lubricin by synoviocytes or superficial zone chondrocytes, depletion of these cells, and/or an elevated breakdown of lubricin. Mice lacking in lubricin exhibit clinical and radiographic manifestations of joint pathology as well as histological irregularities in their articulate joints that become more pronounced as they mature. The most significant characteristics include synovial hyperplasia and subintimal fibrosis, the presence of proteinaceous deposits on the surface of cartilage, irregularities in the cartilage surface and endochondral growth plates, as well as aberrant calcification observed in tendon sheaths and osteophytes [193]. The inclusion of lubricin into an *in vitro* bovine explant cartilage-on-cartilage-bearing system resulted in a considerable reduction in the coefficient of friction and chondrocyte death in the peripheral zone of cartilage. This finding confirmed the essential function played by lubricin in the prevention of cartilage degeneration [194]. The severity of both age-related and post-traumatic osteoarthritis was reduced in transgenic mice by the overproduction of lubricin. The observed decrease can be attributed to the inhibitory effect of lubricin on the expression of genes associated with cartilage breakdown and the enlargement of chondrocytes [191].

4.4. Mechanical Changes

Significant alterations in the functionality of cartilage are observed in individuals with osteoarthritis, leading to negative impacts on the weight-bearing, stabilizing, and lubricating capabilities of articular cartilage.

When subjected to tension, cartilage experiences a loading or stretching force, which causes collagen fibers and entangled proteoglycan molecules to align and elongate in the direction of the applied force. The primary source of resistance to tensile deformation and loads is mostly derived from the inherent stiffness of collagen fibrils [72,195,196].

The tensile modulus in the healthy human articular cartilage has been observed to range between 5 and 25 MPa. This variation depends on factors such as the specific position on the joint surface as well as the depth and orientation of the test specimen in relation to the joint surface [197,198]. The presence of osteoarthritis has been associated with a substantial reduction in the tensile modulus, with a potential loss of up to 90%. This decrease indicates a considerable level of damage to the solid network of cartilage [198]. Likewise, there have been documented reports of reduced tensile stiffness and fracture stress in the human cartilage affected by OA [195,197]. The changes are indicative of structural abnormalities in the collagen fibrillar network, as evidenced by both macroscopic and histological observations. The cartilage affected by degeneration also had a notably higher level of compliance to shear. This phenomenon was related to the presence of fibrillation on the articular surface and the depletion of the extracellular matrix [199]. In their study, Peters et al. [134] observed a significant reduction in the shear storage modulus by around 70–80% compared to the healthy condition.

Previous studies have demonstrated that the articular cartilage exhibiting surface fibrillation, pitting or fraying shows a higher level of compliance or deformability under compression [197,199,200]. Boschetti et al. [139] reported a reduction of 30% in the average thickness and a growth of 8% in the average water levels in OA samples compared to the healthy cartilage. These findings were consistent with the observations made in previous studies [100,155,201,202]. The mechanical properties of OA samples were also evaluated in comparison to those of the healthy cartilage. The static compressive modulus exhibited a decrease of 55–68%. Additionally, the permeability demonstrated an increase of 60–80%, while the dynamic compressive modulus experienced a decrease of 59–64%. Lastly, the static tension modulus displayed a decrease of 72–83% compared to the reference value. According to Armstrong and Mow [100], the compressive modulus of human cartilage tends to decrease as the severity of degeneration increases. Additionally, a reduction in the modulus was observed as individuals progressed in age. On the other hand, it was shown that neither age nor degeneration exhibited any significant variation in hydraulic permeability. Evidently, the OA-induced changes in cartilage, such as fibrillation, heightened hydration, and reduced proteoglycan content, would have a more significant impact on the inherent compressive stiffness of the cartilage compared to its flow-dependent behavior [203].

Ihnatouski et al. [114] observed that there was a decrease in the average values of the instantaneous modulus as the OA grade increased. The osteoarthritis-affected specimens were split into three groups: small, medium, and severely impacted. Young's modulus for the normal cartilage ranged from 1.7 to 0.5 MPa, while the values for the three stages of OA wear were lower—1.14 to 1.3 MPa (small OA), 1.02 to 1.2 MPa (medium OA), and 0.82 to 1.2 MPa (severe OA). Additionally, atomic force microscopy surface-mapping was employed to examine the alterations in surface roughness that occur with an increase in OA stages. The results indicated a positive link between the two variables. Changes in the equilibrium modulus were also investigated. A study by Ebrahimi et al. [204] showed that the tibial plateaus exhibited a significant reduction in E_{eq} , reaching up to 80% compared to the healthy tissue. Similarly, Kleeman et al. [138] discovered that the E_{eq} of cartilage was reduced by around 40% from the early stages to the advanced stages of osteoarthritis.

In a study conducted by Huttu et al. [112], it was observed that mechanical parameters exhibited a negative correlation with cell volume. This relationship was attributed to an increase in the collagen orientation angle inside cartilage as osteoarthritis progressed. Additionally, Nissinen et al. [113] observed significant variations between early and advanced osteoarthritis, leading to a reduction in the initial modulus of the fibril network and the strain-dependent permeability. A positive relationship was observed between the total joint OA grade and the subchondral bone growth [134].

5. Mechanical and Frictional Features of Cartilage Repair Techniques—Are We Getting Close?

The intricate and dynamic nature of hyaline cartilage within the human body poses both challenges and opportunities in the realm of medical science. Cartilage plays a crucial role in maintaining joint function; however, its limited self-repair capability makes cartilage injuries a significant concern for surgeons and scientists. In this section, we will explore the principles, methodologies and outcomes of various cartilage repair techniques, ranging from simple interventions like microfractures to complex tissue-engineering constructs. A summary of the techniques mentioned below is given in Table 2.

5.1. Microfracture

Full-thickness articular cartilage lesions hardly ever heal on their own [93,205]. Numerous techniques have been employed to activate bone marrow in the history of cartilage repair. A complete injury of the hyaline cartilage in a weight-bearing region between the femur and the tibia or in the patellofemoral joint is a common indication for microfracture. The indications for the microfracture technique are usually small lesions up to 2 cm² without subchondral involvement. Exceptionally, it can be used for larger defects (>3 cm²) in less demanding patients [206]. The location of the lesions is also crucial, with much better results achieved at the femoral condyles than at the patellofemoral joint [207]. The microfracture (MFX) technique was extensively researched and developed by Steadman [208,209]. Over the years, advancements [25] have been made in the method, resulting in many improvements. These enhancements include removal of the calcified subchondral bone [210], establishment of straight and uniform cartilage margins [211] and execution of microfractures in close proximity to one another [212]. The perforation of the subchondral bone plate releases liquid bone marrow. Depending on the size of the awl/drill used for bone marrow stimulation, nanofractures with the use of 1 mm drills can be distinguished in this technique. Figure 7 shows the arthroscopic view of the medial femoral condyle with microfractures (MFX). The roughened surface produced by the surgeon provides an area to which the marrow clots can firmly adhere [208,213]. Mesenchymal stromal cells (MSCs) that are introduced into the damaged region have the ability to undergo differentiation into fibrochondrocytes. These fibrochondrocytes then proceed to occupy the defect and subsequently undergo remodeling, resulting in the formation of a fibrocartilage clot [214]. Nevertheless, the abundance of mesenchymal stromal cells is very limited and diminishes with an individual's aging [215]. The composition of the clot primarily consists of type I collagen, which distinguishes it from the natural hyaline cartilage that predominantly comprises type II collagen [216]. Type II collagen possesses a higher concentration of hydroxylysine and a much greater amount of glycosylated hydroxylysine compared to type I collagen. These additional residues might confer distinctive physical characteristics onto type II fibrils [217]. Histological examinations of the tissue-healing process subsequent to microfracture surgery have revealed the predominant presence of fibrocartilage. In other cases, a hybrid repair tissue has been observed, characterized by varying levels of proteoglycan and type II collagen [218,219]. In contrast to hyaline cartilage, fibrocartilage has mechanical qualities that are less optimal for enduring the prolonged stresses associated with joint-loading, owing to its softer nature and lower capacity for tolerating shear stress [220]. The cells present in the fibrous tissue have an elongated phenotype resembling fibroblasts, both in terms of their physical form and the profile of genes they express. The matrix exhibits a reduced concentration of glycosaminoglycans and a higher presence of type I collagen [221,222]. Ebenstein et al. [223] reported that fibrous repair cartilage exhibited a contact stiffness of 0.03 ± 0.01 kN m⁻¹, which was approximately one order of magnitude lower than the contact stiffness of the healthy cartilage (0.17 ± 0.039 kN m⁻¹). The lower compression stiffness could explain the lower resilience of the fibrous repair cartilage to mechanical load [224].

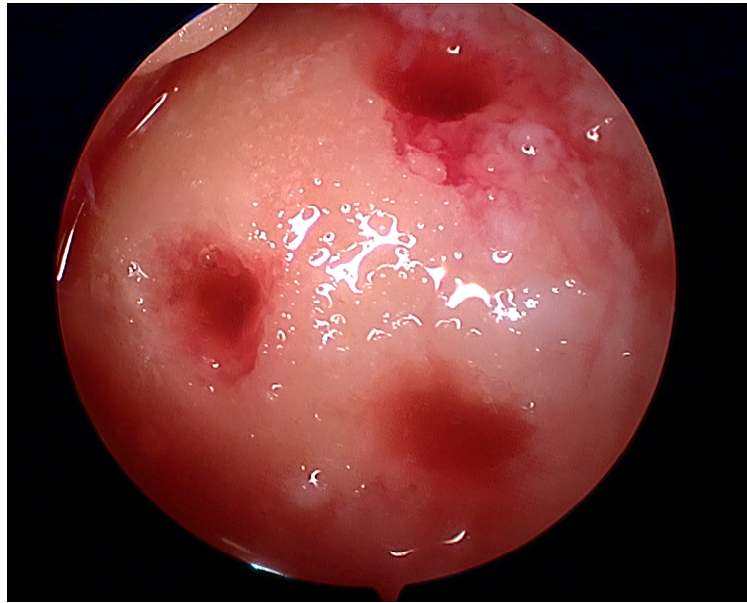


Figure 7. Arthroscopic view of microfractures on the medial femoral condyle. One can appreciate extravagation of bone marrow from the MFX site.

The microfracture technique is frequently used for the treatment of chondral injuries. Nevertheless, like any other surgical procedure, it poses a distinct set of possible risks. Incomplete adhesion or partial filling of the defect by unstable blood clots may lead to poor healing [213]. The occurrence of osseous outgrowth has been observed subsequent to inadvertent removal of the subchondral bone during the operation. Osseous overgrowth occurs frequently, with a reported incidence ranging from 25% to 49% among patients [225,226].

Good short-term clinical results have been reported for the treatment of cartilage lesions using the microfracture technique [227]. However, a longer follow-up indicated steadily decreasing satisfaction with the results and lower durability of the repair over the years [228,229]. Orth et al. [230] in their systematic review reported a failure of rate 11–27% in 5 years of observation and 6–32% during a 10-year period.

5.2. Autologous Matrix-Induced Chondrogenesis (AMIC)

Autologous Matrix-Induced Chondrogenesis (AMIC) is a single-stage procedure for cartilage repair combining microfractures and application of external scaffold. One of the reasons for failure of isolated microfractures may be the lack of protection of the repair site and washing out of MSCs [231]. Adding a matrix allows for stabilization of the clot and provides a scaffold for bone marrow cells, facilitating their differentiation towards the cartilage lineage [232]. Longer follow-up of this technique shows promising results. After 2 years, the outcomes are comparable to isolated microfractures, but after this time, the microfractures are characterized by a decrease in satisfactory results, in contrast to the AMIC technique, which maintains its functional parameters for up to 5 years [229].

5.3. Osteochondral Autograft Transfer System (OATS)

Osteochondral autograft transplantation (OAT) involves the transplantation of grafts obtained from the non-weight-bearing areas of the joint to the injured regions that bear more weight [233]. The application of autograft results in a more expedited and dependable process of osseous integration compared to the osteochondral allograft. Furthermore, the autograft presents several advantages, including convenient accessibility to donor cartilage, capacity for addressing lesions of different sizes, and utilization of the native hyaline cartilage containing functional and fully developed chondrocytes [234,235]. Good results of OATS have been described for small defects (<2 cm²), but larger defects ranging from 2 to 4 cm² can also be treated beneficially with this method, especially in young, demanding

patients [236]. This technique is the first line of treatment for cartilage lesions involving the subchondral layer [234]. The histologic examination of the transplanted osteochondral graft has revealed that in an ideal OATS, the grafts are successfully integrated into the defects to preserve the structural integrity of the hyaline cartilage and cancellous bone. This integration also ensures the maintenance of a smooth and congruent articular surface in the weight-bearing regions [237,238]. Intraoperative views of the OATS procedure are shown in Figures 8 and 9.

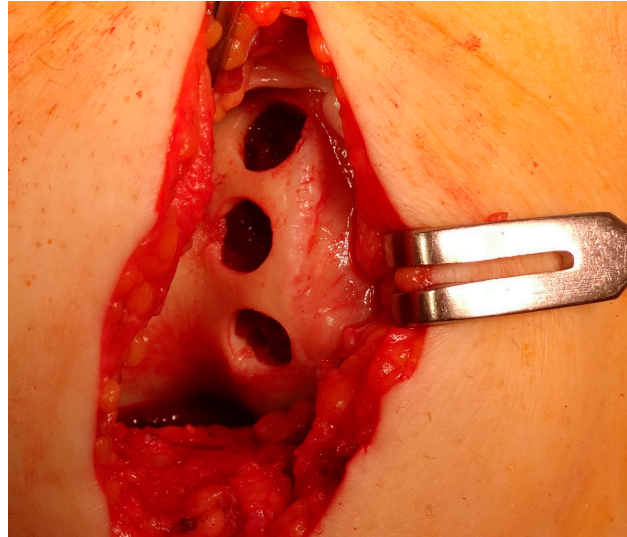


Figure 8. Intraoperative view of donor site preparation for osteochondral blocks implantation on the lateral femoral condyle.

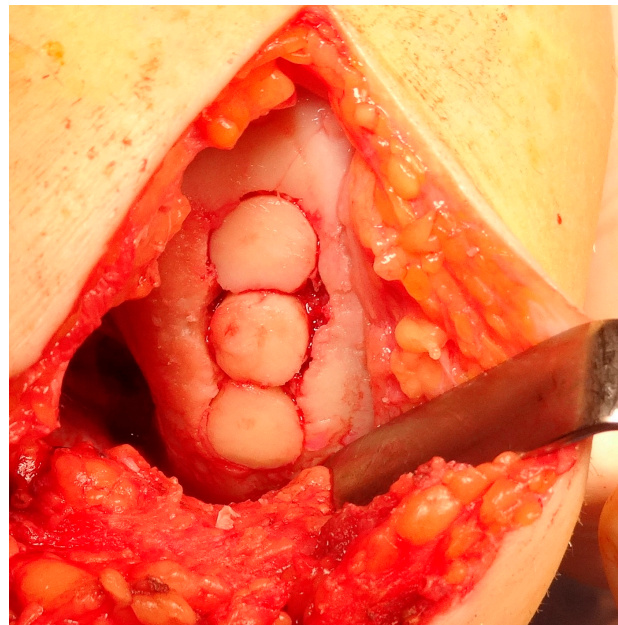


Figure 9. Intraoperative view of the final result with complete cartilage loss area coverage.

Nakaji et al. [239] provided a comprehensive analysis of the progressive alterations in the structural characteristics of an osteochondral cylinder graft–recipient construct. The primary focus of this study was to evaluate the stiffness of articular cartilage using a rabbit model. The articular cartilage stiffness of the osteochondral transplant was within normal parameters upon its first placement ($107,695.1 \pm 11,610.1 \text{ N/m}^2$). During the first, third, and eight weeks following the surgical procedure, it was noticed that the stiffness levels

decreased ($95,386.8 \pm 2689.4$, $92,899.3 \pm 3748.2$, and $95,969.8 \pm 2157.1$ N/m², respectively) compared to the stiffness typically detected in healthy cartilage ($100,027.5 \pm 396.4$ N/m²). Additionally, the histological analysis revealed an increase in the bone trabeculae inside the subchondral region. At the 12-week post-operative mark, the articular cartilage of the osteochondral graft exhibited normal stiffness ($104,683.7 \pm 3311.5$ N/m²), and the bone trabeculae in the subchondral region demonstrated effective remodeling.

A study by Kuroki et al. [240] investigated the mechanical impact of an OATS on articular cartilage in a porcine model. They employed an ultrasonic measurement system to assess the immediate post-surgical outcomes. The findings of the study indicated that the surgical procedure of osteochondral grafting did not induce any significant alterations in the stiffness (9.2 ± 1.78 and 9.0 ± 1.91 [corresponding values, mean \pm SD] before harvesting and after grafting, respectively, in a 6 mm-plug model and 5.8 ± 1.54 and 5.8 ± 1.87 , respectively, in a 5 mm-plug model), surface irregularity (0.7 ± 0.10 μ seconds and 0.7 ± 0.11 μ seconds, before harvesting and after grafting, respectively, in a 6 mm-plug and 0.8 ± 0.12 μ seconds and 0.8 ± 0.09 μ seconds, respectively, in a 5 mm-plug model), or thickness of the graft plug (2.7 ± 0.57 μ seconds and 2.7 ± 0.62 μ seconds, before harvesting and after grafting, respectively, in a 6 mm-plug model and 2.4 ± 0.81 m seconds and 2.3 ± 0.67 m seconds, respectively, in a 5 mm-plug model). Additionally, it was hypothesized that in the event of mechanical alterations, a change in stiffness would be more likely related to the healing or remodeling process rather than to the surgical procedure.

Lane et al. [241] examined the biochemical and biomechanical alterations throughout a goat osteochondral autograft model after 12 weeks following surgery. The stiffness of the healthy cartilage was 0.79 ± 0.15 N/mm, whereas the cartilage of the transferred plugs ranged 5.29 ± 1.04 N/mm. This indicated that the graft cartilage had a stiffness that was 6 to 7 times larger than that of the control normal tissue. Moreover, viability of the cells in the bone plugs were examined by confocal microscopy. In total, 95% of the cells counted manually were viable 12 weeks after grafting. The assessment of the joint surfaces showed no significant degenerative changes at either the recipient or the donor locations 12 weeks post implantation.

The biomechanical and histological characteristics of the OATS were also investigated by Nam et al. [242] in a rabbit model. The stiffness of the 12-week grafts (1213.6 ± 309.0 N/mm) was found to be substantially greater than that of the 6-week grafts (483.1 ± 229.1 N/mm) and natural cartilage (774.8 ± 117.1 N/mm). The stiffness of the grafts at the 6-week mark revealed a statistically significant reduction in comparison to the stiffness observed in the natural cartilage. Furthermore, with regard to a potential score of 24.0 points, the average values for the overall healing indices (Modified O'Driscoll Histological Score) [243] were as follows: 6-week OAT, 21.6 ± 1.3 ; 12-week OAT, 21.0 ± 1.8 ; 6-week full-thickness defects, 11.5 ± 2.8 ; and 12-week full-thickness defects, 10.8 ± 4.4 . The histology scores of the OAT groups were considerably superior compared to the full-thickness defects groups in both time periods.

The successful use of autograft is subject to some constraints, with defect size being the primary one. Lesions above 3 cm² in size are susceptible to experiencing symptomatic donor-site morbidity, resulting in pain and associated symptoms [244]. The rate of donor-site morbidity has been reported to range from 2.3% to 12.6% [245,246]. However, OATS has very good long-term clinical results with functional benefits and survival beyond 15 years [247].

5.4. Autologous Chondrocyte Implantation—ACI

The Autologous Chondrocyte Implantation (ACI) procedure was first introduced in 1994 [205]. It involves a two-step approach, beginning with the collection of a sample of the patient's articular cartilage in the first stage. Subsequently, after *ex vivo* multiplication, the cells are inserted to the chondral defect during the second stage. The ACI possesses the notable benefit of effectively addressing extensive lesions measuring up to 10 cm²

by the restoration of cartilage that closely resembles hyaline cartilage [248–252]. The growth of hyaline-like tissue during the healing of chondral lesions is expected to yield biomechanical qualities that are comparable to those of the healthy cartilage, as shown by stiffness measures [250]. The grafted area's stiffness was measured to be 2.4 ± 0.3 N, while the normal cartilage's result was 3.2 ± 0.3 N. Moreover, the average stiffness measurement in the grafted sections containing hyaline tissue was found to be 3.0 ± 1.1 , whereas a stiffness of 1.5 ± 0.35 was reported in the repairs involving fibrous tissue. In 8 out of 12 cases of stiffness testing, the indentation measurement exhibited a value that was equal to or more than 90% of the value seen in the healthy cartilage.

According to Vasara et al. [252], the stiffness of the repaired tissue exhibited a notable increase, reaching 62% of the stiffness observed in the surrounding cartilage. The indentation force of the repair tissue in six individuals was shown to exceed 80% of the adjacent cartilage, indicating a potential presence of hyaline-like repair. The mean indentation force of the repair tissue was 2.04 ± 0.83 N, which accounted for 62% of the adjacent cartilage (3.58 ± 1.04 N). However, it is important to note that there was a significant difference in the stiffness of the repair tissue.

Henderson et al. [253] conducted an evaluation of 66 ACI repairs for articular cartilage injuries. The mean normalized stiffness for the entire sample of 66 lesions was found to be 104% at an average follow-up period of 22.1 months post-implantation. A notable observation was made regarding the stiffness of both hyaline articular cartilage and hyaline-like repairs, with about half of these samples exhibiting greater stiffness compared to the adjacent cartilage. It was suggested that it could be due to the difference in matrix composition during the healing process. The alteration in cartilage matrix composition occurring with the aging process may differ from the repair composition that more closely approaches the stiffer structure often observed in children. On the other hand, it is possible that a higher repair stiffness would lead to the occurrence of symptomatic repair due to abnormal load transmission, which is comparable to the reported high stiffness of the subchondral bone plate in individuals with OA. Hence, the increased stiffness might have negative implications for joint functionality. Moreover, based on the clinical and arthroscopic observations, repairs were categorized into two groups: ACI-unrelated problems (Group A) and ACI-related problems (Group B). In Group A, a majority of repairs, namely 65%, consisted of either hyaline or hyaline-like cartilage, but in Group B this proportion was significantly lower and amounted to 28%. Autologous chondrocyte repairs consisting of fibrocartilage had a higher prevalence of morphologic defects and manifested symptoms at an earlier stage compared to the repairs using hyaline or hyaline-like cartilage. The reparative characteristics of hyaline articular cartilage were shown to have biomechanical parameters that were equivalent to the adjacent cartilage and higher than those observed for fibrocartilage repairs.

Despite initial good clinical results, ACI is characterized by a higher rate of complications, such as periosteal patch hypertrophy, high reoperation rates, bulky sutures, and cell leakage [254]. The occurrence of such adverse effects paved the way for the matrix-based modification of this technique using matrix-induced autologous chondrocyte implantation (MACI).

5.5. Matrix-Induced Autologous Chondrocyte Implantation—MACI

MACI is a more recent variation of ACI, which incorporates a collagen scaffold to facilitate the use of autologous cells and promote directed tissue regeneration. This next-generation method has the advantage of utilizing the patient's own cells while employing a biocompatible scaffold made of collagen. A surgical visualization via a dry arthroscopy technique is shown in Figure 10. The MACI implant possesses intrinsic benefits such as the ability to be surgically implanted by arthroscopy or miniarthrotomy, no periosteal harvest, and its utilization of tissue adhesive as a substitute for sutures [255]. The efficacy of MACI has been assessed in many animal experiments, demonstrating its ability to enhance the healing process in full-thickness cartilage injuries. The immunological or

inflammatory responses elicited by the membrane alone have been assessed and shown to be modest [256,257]. MACI is indicated as a first line of treatment for lesions above 2 cm² and second for defects below 2 cm² [258].



Figure 10. Dry arthroscopy view of a biodegradable non-woven hyaluronic acid scaffold covering a cartilage defect on the medial femoral condyle.

A study by Lee et al. [259] demonstrated that the use of a MACI graft in combination with a type II collagen membrane resulted in an aggregate modulus that was 15% of the modulus observed in the native tissue. The results of stiffness tests conducted on an ovine model demonstrated that the MACI grafts exhibited a stiffness range of 16% to 50% in comparison to the natural cartilage [256,260].

Griffin et al. [261] investigated the mechanical characteristics of MACI cartilage repair in an equine model. The findings indicated that the compressive and frictional properties of the repaired tissue were comparable to those of the natural tissue. The equilibrium modulus of the cartilage obtained from the defects that underwent MACI was found to be 70% of that observed in the normal cartilage. This value was not found to have a statistically significant difference when compared to the equilibrium modulus of the native control tissue. Moreover, there was no statistically significant difference between the control tissue and the implant groups in terms of the average values of boundary mode friction coefficients which varied from 0.42 to 0.52. The shear modulus values for the healthy cartilage generally varied between 1.0 and 1.5 MPa; however, the shear moduli of the cartilage from all categories of injuries were much lower, ranging from 0.2 to 0.5 MPa, which represents a reduction of 4 to 10 times compared to the healthy cartilage. The low shear modulus of the grafts made the restored cartilage vulnerable to mechanical failure or deterioration.

Schuetz et al. [262] reported favorable mid- to long-term clinical results of the MACI technique. It significantly increased patient-related scores (KOOS, SF-36, Tegner). Comparison of MFX and MACI at 5-year follow-up shows significantly better results in the KOOS pain score and functional scales and non-significantly lower risk of failure [205].

5.6. Tissue Engineering

The concept of osteochondral and cartilage tissue engineering has emerged as a means to forward the development of novel and enhanced therapeutic interventions. There exist two primary approaches to the restoration of impaired osteochondral modulus and complete-thickness cartilage through the use of tissue-engineering techniques. The objective is to create artificial cartilage structures that replicate the structural characteristics,

mechanical attributes and, therefore, biological functionalities of natural cartilage tissues. An alternative approach puts greater emphasis on the field of regenerative medicine. The fundamental idea revolves around the administration of suitable biomaterials in the form of artificial extracellular matrix to stimulate cellular growth, proliferation, and differentiation at the injury zone. This approach relies on the inherent biological processes involving cellular interactions and biomolecules to facilitate the regeneration of articular cartilage and subchondral bone [263]. An implantation of the collagen matrix with a preparation of the donor site is shown in Figures 11 and 12.



Figure 11. Dry arthroscopy view of a full-thickness cartilage injury in the femoral trochlea after debridement and preparation for matrix implantation.



Figure 12. Dry arthroscopy view of the same defect filled with cell-free matrix gel.

Koh et al. [264] utilized the finite element analysis to demonstrate the efficacy of a scaffold with ideal mechanical qualities in promoting cartilage regeneration within a cartilage defect. It was assumed that the implantation of a scaffold with ideal mechanical qualities would serve to mitigate cell death and promote increased development of cartilage tissue.

The scaffolds utilized in cartilage tissue engineering are mostly composed of carbohydrates such as alginate, chitosan, poly-L-lactide/poly(glycolic acid) (PLLA/PGA),

agarose, and hyaluronic acid, as well as proteins like collagen and gelatin. Growth factors are employed to induce the proliferation and differentiation of cells that will be transplanted onto the scaffold, hence promoting the maintenance of their chondrogenic phenotype [265]. Other authors have explored alternative mechanical and chemical stimuli in pre-implantation culture in order to enhance lubrication efficiency [266]. Scaffolds which are better-structured present higher elastic values [267].

Hydrogels are polymer networks that exhibit a three-dimensional structure characterized by significant swelling and porosity at the molecular level. This unique structure enables the transport of diverse solutes and nutrients inside the hydrogel matrix. The fabricated structure possesses cell compatibility, enabling the containment of various cell types such as chondrocytes and stromal cells. Moreover, a variety of hydrogel characteristics may be adjusted to enhance their effectiveness in tissue regeneration. These parameters encompass polymer chemistry, crosslinking density, degradation, mechanical qualities, and release kinetics of biological components [268]. Hydrogels with reduced crosslinking density exhibit lower mechanical properties. Dynamic loading conditions have the potential to promote the process of chondrogenesis in mesenchymal stromal cells [268,269]. The mechanical strength of natural hydrogel scaffolds can vary between 0.45 and 5.65 MPa, but synthetic hydrogels have the potential to reach values ranging from 15 to 125 MPa [270].

When compared to solid scaffolds, hydrogels facilitate the adoption of a more spherical shape by cells, which is a hallmark feature of the chondrogenic phenotype. This, in turn, leads to a reduction in the production of fibrous tissues [271]. However, hydrogels have restricted mechanical characteristics, which renders them susceptible to failure. This drawback poses a significant disadvantage, particularly considering that articular cartilage is exposed to substantial mechanical pressures. Furthermore, it should be noted that these particular materials still exhibit limitations in their capacity for effective integration with the adjacent tissues [272].

Also worth highlighting in this paper is the need for adequate oxygen concentration during chondrocyte culturing [273–275]. It has been proven that a physiological (5%) oxygen concentration while culturing chondrocytes promotes proper and adequate chondrogenesis. An optimal oxygen concentration increases GAG production, therefore increasing compressive strength of the constructs [276]. Physioxia during chondrocyte culturing also promotes collagen type II production [277].

Table 2. Comparison of the biomechanical properties of different cartilage repair methods.

Study	Operative Technique	Tissue Type	Measurement System	Biomechanical Results	Additional Findings
Ebenstein et al. [223]	MFx	Animal model—rabbits	Nanoindentation	Stiffness 0.03 ± 0.01 kN m ⁻¹ —fibrous repair 0.17 ± 0.039 kN m ⁻¹ —normal cartilage	
Nakaji et al. [239]	OATS	Animal model—rabbits	Tactile frequency	Stiffness 107,695.1 ± 11,610.1 N/m ² after procedure; 95,386.8 ± 2689.4 after 1 week; 92,899.3 ± 3748.2 after 3 weeks; 95,969.8 ± 2157.1 N/m ² after 8 weeks; 104,683.7 ± 3311.5 N/m ² after 12 weeks 100,027.5 ± 396.4 N/m ² —normal cartilage	Increase in bone trabeculae inside the subchondral region.

Table 2. Cont.

Study	Operative Technique	Tissue Type	Measurement System	Biomechanical Results	Additional Findings
Kuroki et al. [240]	OATS	Animal model—porcine	Ultrasonic	Stiffness 9.2 ± 1.78 (before harvesting) and 9.0 ± 1.91 (after grafting) [corresponding values]—6 mm plug model 5.8 ± 1.54 (before harvesting) and 5.8 ± 1.87 (after grafting)—5 mm plug model	Changes in stiffness are more likely related to the healing or remodeling process rather than to the surgical procedure
Lane et al. [241]	OATS	Animal model—goats	Indentation	Stiffness 5.29 ± 1.04 N/mm—transferred plugs after 12 weeks 0.79 ± 0.15 N/mm—normal cartilage	In total, 95% of the cells counted manually by confocal microscopy were viable 12 weeks after transfer
Nam et al. [242]	OATS	Animal model—rabbits	Indentation	Stiffness 1213.6 ± 309.0 N/mm—12 weeks after transplant 483.1 ± 229.1 N/mm—6 weeks after transplant 774.8 ± 117.1 N/mm—normal cartilage	Modified O'Driscoll Histological Score (24 points max): 6-week OAT, 21.6 ± 1.3; 12-week OAT, 21.0 ± 1.8; 6-week full-thickness defects, 11.5 ± 2.8; 12-week full-thickness defects, 10.8 ± 4.4
Hangody et al. [237]	OATS	Human	Arthroscopic Indentation	Stiffness Stiffness of the resurfaced area similar to the surrounding hyaline cartilage (no numerical data)	
Peterson et al. [250]	ACI	Human	Indentation	Stiffness 2.4 ± 0.3 N—grafted area 3.2 ± 0.3 N—normal cartilage 3.0 ± 1.1 N—mean value at hyaline repair 1.5 ± 0.35—mean value at fibrous repair	
Vasara et al. [252]	ACI	Human	Indentation	Stiffness 2.04 ± 0.83 N—repair tissue 3.58 ± 1.04 N—normal cartilage	
Henderson et al. [253]	ACI	Human	Arthroscopic Indentation	Stiffness 3 ± 1.5 N—maximum stiffness of the repair Avg. normalized stiffness—104% of the surrounding hyaline cartilage	
Lee et al. [259]	MACI	Animal model—canine	Indentation	Aggregate modulus 15% of the native cartilage	

Table 2. Cont.

Study	Operative Technique	Tissue Type	Measurement System	Biomechanical Results	Additional Findings
Griffin et al. [261]	MACI	Animal model—equine	Custom tribometer	Avg. values of boundary mode friction coefficients—from 0.42 to 0.52 Shear modulus 0.2 to 0.5 MPa—repaired cartilage 1.0 to 1.5 MPa—normal cartilage	
Franke et al. [220]	MACI (periosteal cells)	Animal model—miniature pigs	Nanoindentation	Stiffness 0.5 kN m ⁻¹ —repaired cartilage 4.0 kN m ⁻¹ —normal cartilage	
Tanaka et al. [267]	Tissue Engineering	PLLA scaffolds	Indentation	Elastic moduli 3000–28,000 kPa	

6. Conclusions

As shown in this review, the articular cartilage is one of the most sophisticated tissues in human body. Although it can withstand various forces without harm, once injured, it gives rise to the development of osteoarthritis due to ECM breakdown, resulting in increased load transmitted to the subchondral bone. This review has also demonstrated the impact of various mechanical and tribological properties on cartilage deterioration and repair techniques. Out of the mentioned repair techniques, OATS showed the closest resemblance to the native hyaline cartilage with regard to mechanical properties. This is attributed to the healthy subchondral bone, which is implemented with the overlying cartilage. Cartilage repair techniques which do not utilize subchondral bone, such as ACI and MACI, showed a decrease in mechanical properties, especially in shear modulus and stiffness. On the other hand, these are techniques which do not require harvesting of high-volume healthy cartilage to fill the defect. Up to date, there is no strong consensus regarding cartilage repair methods and mechanical testing. Therefore, more studies are required to find the best solution for the patient. In future, not only mechanical properties but also signaling pathways and inflammation modulation will play a role in finding the best solution for cartilage repair.

Author Contributions: Conceptualization, P.K. and R.K.; methodology, A.R. and J.S.; validation, P.K. and R.K.; formal analysis, P.K.; investigation, A.R. and J.S.; resources, A.R. and J.S.; writing—original draft preparation, P.K., A.R., J.S. and R.K.; writing—review and editing, P.K. and R.K.; visualization, A.R. and J.S.; supervision, P.K. and R.K.; funding acquisition, P.K. All authors have read and agreed to the published version of the manuscript.

Funding: The APC was funded by Carolina Medical Center.

Institutional Review Board Statement: Not applicable.

Informed Consent Statement: Not applicable.

Data Availability Statement: Not applicable.

Conflicts of Interest: The authors declare no conflict of interest.

References

1. Quicke, J.G.; Conaghan, P.G.; Corp, N.; Peat, G. Osteoarthritis Year in Review 2021: Epidemiology & Therapy. *Osteoarthr. Cartil.* **2022**, *30*, 196–206. [CrossRef]
2. Krakowski, P.; Karpiński, R.; Maciejewski, R.; Jonak, J. Evaluation of the Diagnostic Accuracy of MRI in Detection of Knee Cartilage Lesions Using Receiver Operating Characteristic Curves. *J. Phys. Conf. Ser.* **2021**, *1736*, 012028. [CrossRef]

3. Karpiński, R.; Krakowski, P.; Jonak, J.; Machrowska, A.; Maciejewski, M. Comparison of Selected Classification Methods Based on Machine Learning as a Diagnostic Tool for Knee Joint Cartilage Damage Based on Generated Vibroacoustic Processes. *Appl. Comput. Sci.* **2023**, *19*, 136–150. [[CrossRef](#)]
4. Long, H.; Liu, Q.; Yin, H.; Wang, K.; Diao, N.; Zhang, Y.; Lin, J.; Guo, A. Prevalence Trends of Site-Specific Osteoarthritis From 1990 to 2019: Findings From the Global Burden of Disease Study 2019. *Arthritis Rheumatol.* **2022**, *74*, 1172–1183. [[CrossRef](#)]
5. Machrowska, A.; Karpiński, R.; Maciejewski, M.; Jonak, J.; Krakowski, P. Application of Eemd-Dfa Algorithms and Ann Classification for Detection of Knee Osteoarthritis Using Vibroarthrography. *Appl. Comput. Sci.* **2024**, *20*, 90–108. [[CrossRef](#)]
6. Reyes, C.; Garcia-Gil, M.; Elorza, J.; Mendez-Boo, L.; Hermosilla, E.; Javaid, M.; Cooper, C.; Diez-Perez, A.; Arden, N.; Bolibar, B.; et al. Socio-Economic Status and the Risk of Developing Hand, Hip or Knee Osteoarthritis: A Region-Wide Ecological Study. *Osteoarthr. Cartil.* **2015**, *23*, 1323–1329. [[CrossRef](#)]
7. Johnson, V.; Hunter, D. The Epidemiology of Osteoarthritis. *Best. Pract. Res. Clin. Rheumatol.* **2014**, *28*, 5–15. [[CrossRef](#)]
8. Van Buuren, M.M.A.; Arden, N.K.; Bierma-Zeinstra, S.M.A.; Bramer, W.M.; Casartelli, N.C.; Felson, D.T.; Jones, G.; Lane, N.E.; Lindner, C.; Maffiuletti, N.A.; et al. Statistical Shape Modeling of the Hip and the Association with Hip Osteoarthritis: A Systematic Review. *Osteoarthr. Cartil.* **2021**, *29*, 607–618. [[CrossRef](#)]
9. Hunter, D.J.; Schofield, D.; Callander, E. The Individual and Socioeconomic Impact of Osteoarthritis. *Nat. Rev. Rheumatol.* **2014**, *10*, 437–441. [[CrossRef](#)]
10. Hunter, D.J.; Bierma-Zeinstra, S. Osteoarthritis. *Lancet* **2019**, *393*, 1745–1759. [[CrossRef](#)]
11. Cibere, J.; Sayre, E.C.; Guermazi, A.; Nicolaou, S.; Kopec, J.A.; Esdaile, J.M.; Thorne, A.; Singer, J.; Wong, H. Natural History of Cartilage Damage and Osteoarthritis Progression on Magnetic Resonance Imaging in a Population-Based Cohort with Knee Pain. *Osteoarthr. Cartil.* **2011**, *19*, 683–688. [[CrossRef](#)]
12. Lin, W.; Klein, J. Recent Progress in Cartilage Lubrication. *Adv. Mater.* **2021**, *33*, 2005513. [[CrossRef](#)] [[PubMed](#)]
13. Karpiński, R. Knee Joint Osteoarthritis Diagnosis Based on Selected Acoustic Signal Discriminants Using Machine Learning. *Appl. Comput. Sci.* **2022**, *18*, 71–85. [[CrossRef](#)]
14. Karpiński, R.; Krakowski, P.; Jonak, J.; Machrowska, A.; Maciejewski, M.; Nogalski, A. Diagnostics of Articular Cartilage Damage Based on Generated Acoustic Signals Using ANN—Part I: Femoral-Tibial Joint. *Sensors* **2022**, *22*, 2176. [[CrossRef](#)] [[PubMed](#)]
15. Machrowska, A.; Karpiński, R.; Maciejewski, M.; Jonak, J.; Krakowski, P.; Syta, A. Application of Recurrence Quantification Analysis in the Detection of Osteoarthritis of the Knee with the Use of Vibroarthrography. *Adv. Sci. Technol. Res. J.* **2024**, *18*, 19–31. [[CrossRef](#)]
16. Torzilli, P.A.; Allen, S.N. Effect of Articular Surface Compression on Cartilage Extracellular Matrix Deformation. *J. Biomech. Eng.* **2022**, *144*, 091007. [[CrossRef](#)] [[PubMed](#)]
17. Zappone, B.; Greene, G.W.; Oroudjev, E.; Jay, G.D.; Israelachvili, J.N. Molecular Aspects of Boundary Lubrication by Human Lubricin: Effect of Disulfide Bonds and Enzymatic Digestion. *Langmuir* **2008**, *24*, 1495–1508. [[CrossRef](#)] [[PubMed](#)]
18. Ghosh, S.; Abanteriba, S. Status of Surface Modification Techniques for Artificial Hip Implants. *Sci. Technol. Adv. Mater.* **2016**, *17*, 715–735. [[CrossRef](#)] [[PubMed](#)]
19. Gleghorn, J.P.; Jones, A.R.C.; Flannery, C.R.; Bonassar, L.J. Alteration of Articular Cartilage Frictional Properties by Transforming Growth Factor Beta, Interleukin-1beta, and Oncostatin M. *Arthritis Rheum.* **2009**, *60*, 440–449. [[CrossRef](#)] [[PubMed](#)]
20. Karpiński, R.; Machrowska, A.; Maciejewski, M. Application of Acoustic Signal Processing Methods in Detecting Differences between Open and Closed Kinematic Chain Movement for the Knee Joint. *Appl. Comput. Sci.* **2019**, *15*, 36–48. [[CrossRef](#)]
21. Filardo, G.; Previtali, D.; Napoli, F.; Candrian, C.; Zaffagnini, S.; Grassi, A. PRP Injections for the Treatment of Knee Osteoarthritis: A Meta-Analysis of Randomized Controlled Trials. *Cartilage* **2021**, *13*, 364S–375S. [[CrossRef](#)] [[PubMed](#)]
22. Volpi, N. Chondroitin Sulfate Safety and Quality. *Molecules* **2019**, *24*, 1447. [[CrossRef](#)] [[PubMed](#)]
23. van Doormaal, M.C.M.; Meerhoff, G.A.; Vliet Vlieland, T.P.M.; Peter, W.F. A Clinical Practice Guideline for Physical Therapy in Patients with Hip or Knee Osteoarthritis. *Musculoskelet. Care* **2020**, *18*, 575–595. [[CrossRef](#)] [[PubMed](#)]
24. Peck, J.; Slovek, A.; Miro, P.; Vij, N.; Traube, B.; Lee, C.; Berger, A.A.; Kassem, H.; Kaye, A.D.; Sherman, W.F.; et al. A Comprehensive Review of Viscosupplementation in Osteoarthritis of the Knee. *Orthop. Rev.* **2021**, *13*, 25549. [[CrossRef](#)] [[PubMed](#)]
25. Krakowski, P.; Karpiński, R.; Maciejewski, R.; Jonak, J.; Jurkiewicz, A. Short-Term Effects of Arthroscopic Microfracturation of Knee Chondral Defects in Osteoarthritis. *Appl. Sci.* **2020**, *10*, 8312. [[CrossRef](#)]
26. Liu, X.; Chen, Z.; Gao, Y.; Zhang, J.; Jin, Z. High Tibial Osteotomy: Review of Techniques and Biomechanics. *J. Healthc. Eng.* **2019**, *2019*, 8363128. [[CrossRef](#)]
27. Bhattacharjee, M.; Coburn, J.; Centola, M.; Murab, S.; Barbero, A.; Kaplan, D.L.; Martin, I.; Ghosh, S. Tissue Engineering Strategies to Study Cartilage Development, Degeneration and Regeneration. *Adv. Drug Deliv. Rev.* **2015**, *84*, 107–122. [[CrossRef](#)] [[PubMed](#)]
28. Kwon, H.; Brown, W.E.; Lee, C.A.; Wang, D.; Paschos, N.; Hu, J.C.; Athanasiou, K.A. Surgical and Tissue Engineering Strategies for Articular Cartilage and Meniscus Repair. *Nat. Rev. Rheumatol.* **2019**, *15*, 550–570. [[CrossRef](#)] [[PubMed](#)]
29. Firestein, G.S.; Kelley, W.N. *Kelley's Textbook of Rheumatology*, 8th ed.; Saunders Elsevier: Philadelphia, PA, USA, 2009.
30. Guo, J.; Yan, P.; Qin, Y.; Liu, M.; Ma, Y.; Li, J.; Wang, R.; Luo, H.; Lv, S. Automated Measurement and Grading of Knee Cartilage Thickness: A Deep Learning-Based Approach. *Front. Med.* **2024**, *11*, 1337993. [[CrossRef](#)]
31. Hunziker, E.B.; Quinn, T.M.; Häuselmann, H.-J. Quantitative Structural Organization of Normal Adult Human Articular Cartilage. *Osteoarthr. Cartil.* **2002**, *10*, 564–572. [[CrossRef](#)]

32. Alford, J.W.; Cole, B.J. Cartilage Restoration, Part 1: Basic Science, Historical Perspective, Patient Evaluation, and Treatment Options. *Am. J. Sports Med.* **2005**, *33*, 295–306. [[CrossRef](#)]
33. Musculoskeletal Regeneration Program, AO Research Institute Davos, Clavadelerstrasse 8, CH-7270 Davos Platz, Switzerland; Schätti, O.; Grad, S.; Goldhahn, J.; Salzmann, G.; Li, Z.; Alini, M.; Stoddart, M. A Combination of Shear and Dynamic Compression Leads to Mechanically Induced Chondrogenesis of Human Mesenchymal Stem Cells. *Eur. Cell. Mater.* **2011**, *22*, 214–225. [[CrossRef](#)]
34. Sah, R.L.-Y.; Kim, Y.; Doong, J.H.; Grodzinsky, A.J.; Plass, A.H.K.; Sandy, J.D. Biosynthetic Response of Cartilage Explants to Dynamic Compression. *J. Orthop. Res.* **1989**, *7*, 619–636. [[CrossRef](#)]
35. Gray, M.L.; Pizzanelli, A.M.; Grodzinsky, A.J.; Lee, R.C. Mechanical and Physicochemical Determinants of the Chondrocyte Biosynthetic Response. *J. Orthop. Res.* **1988**, *6*, 777–792. [[CrossRef](#)]
36. Sophia Fox, A.J.; Bedi, A.; Rodeo, S.A. The Basic Science of Articular Cartilage. *Sports Health* **2009**, *1*, 461–468. [[CrossRef](#)]
37. Krakowski, P.; Nogalski, A.; Jurkiewicz, A.; Karpiński, R.; Maciejewski, R.; Jonak, J. Comparison of Diagnostic Accuracy of Physical Examination and MRI in the Most Common Knee Injuries. *Appl. Sci.* **2019**, *9*, 4102. [[CrossRef](#)]
38. Muir, H. The Chondrocyte, Architect of Cartilage. Biomechanics, Structure, Function and Molecular Biology of Cartilage Matrix Macromolecules. *Bioessays* **1995**, *17*, 1039–1048. [[CrossRef](#)]
39. Buckwalter, J.A.; Mow, V.C.; Ratcliffe, A. Restoration of Injured or Degenerated Articular Cartilage. *J. Am. Acad. Orthop. Surg.* **1994**, *2*, 192–201. [[CrossRef](#)]
40. Karpiński, R.; Krakowski, P.; Jonak, J.; Machrowska, A.; Maciejewski, M.; Nogalski, A. Diagnostics of Articular Cartilage Damage Based on Generated Acoustic Signals Using ANN—Part II: Patellofemoral Joint. *Sensors* **2022**, *22*, 3765. [[CrossRef](#)] [[PubMed](#)]
41. Eschweiler, J.; Horn, N.; Rath, B.; Betsch, M.; Baroncini, A.; Tingart, M.; Migliorini, F. The Biomechanics of Cartilage—An Overview. *Life* **2021**, *11*, 302. [[CrossRef](#)] [[PubMed](#)]
42. Chery, D.R.; Han, B.; Zhou, Y.; Wang, C.; Adams, S.M.; Chandrasekaran, P.; Kwok, B.; Heo, S.-J.; Enomoto-Iwamoto, M.; Lu, X.L.; et al. Decorin Regulates Cartilage Pericellular Matrix Micromechanobiology. *Matrix Biol.* **2021**, *96*, 1–17. [[CrossRef](#)]
43. Rexwinkle, J.T.; Hunt, H.K.; Pfeiffer, F.M. Characterization of the Surface and Interfacial Properties of the Lamina Splendens. *Front. Mech. Eng.* **2017**, *12*, 234–252. [[CrossRef](#)]
44. Thambyah, A.; Broom, N. On How Degeneration Influences Load-Bearing in the Cartilage–Bone System: A Microstructural and Micromechanical Study. *Osteoarthr. Cartil.* **2007**, *15*, 1410–1423. [[CrossRef](#)]
45. Hollander, A.P.; Pidoux, I.; Reiner, A.; Rorabeck, C.; Bourne, R.; Poole, A.R. Damage to Type II Collagen in Aging and Osteoarthritis Starts at the Articular Surface, Originates around Chondrocytes, and Extends into the Cartilage with Progressive Degeneration. *J. Clin. Investig.* **1995**, *96*, 2859–2869. [[CrossRef](#)]
46. Hollander, A.P.; Dickinson, S.C.; Sims, T.J.; Brun, P.; Cortivo, R.; Kon, E.; Marcacci, M.; Zanasi, S.; Borriore, A.; Luca, C.D.; et al. Maturation of Tissue Engineered Cartilage Implanted in Injured and Osteoarthritic Human Knees. *Tissue Eng.* **2006**, *12*, 1787–1798. [[CrossRef](#)]
47. Gottardi, R.; Hansen, U.; Raiteri, R.; Loparic, M.; Düggelin, M.; Mathys, D.; Friederich, N.F.; Bruckner, P.; Stolz, M. Supramolecular Organization of Collagen Fibrils in Healthy and Osteoarthritic Human Knee and Hip Joint Cartilage. *PLoS ONE* **2016**, *11*, e0163552. [[CrossRef](#)]
48. Eyre, D.R.; Wu, J.J. Collagen Structure and Cartilage Matrix Integrity. *J. Rheumatol. Suppl.* **1995**, *43*, 82–85.
49. Bayliss, M.T.; Ali, S.Y. Age-related changes in the composition and structure of human articular-cartilage proteoglycans. *Biochem. J.* **1978**, *176*, 683–693. [[CrossRef](#)]
50. Knudson, C.B.; Knudson, W. Cartilage Proteoglycans. *Semin. Cell Dev. Biol.* **2001**, *12*, 69–78. [[CrossRef](#)]
51. Venn, M.; Maroudas, A. Chemical Composition and Swelling of Normal and Osteoarthrotic Femoral Head Cartilage. I. *Chem. Compos. Ann. Rheum. Dis.* **1977**, *36*, 121–129. [[CrossRef](#)] [[PubMed](#)]
52. Fujie, H.; Imade, K. Effects of Low Tangential Permeability in the Superficial Layer on the Frictional Property of Articular Cartilage. *Biosurface Biotribology* **2015**, *1*, 124–129. [[CrossRef](#)]
53. Flannery, C.R.; Hughes, C.E.; Schumacher, B.L.; Tudor, D.; Aydelotte, M.B.; Kuettner, K.E.; Caterson, B. Articular Cartilage Superficial Zone Protein (SZP) Is Homologous to Megakaryocyte Stimulating Factor Precursor and Is a Multifunctional Proteoglycan with Potential Growth-Promoting, Cytoprotective, and Lubricating Properties in Cartilage Metabolism. *Biochem. Biophys. Res. Commun.* **1999**, *254*, 535–541. [[CrossRef](#)]
54. Styczynska-Soczka, K.; Amin, A.K.; Hall, A.C. Cell-Associated Type I Collagen in Nondegenerate and Degenerate Human Articular Cartilage. *J. Cell. Physiol.* **2021**, *236*, 7672–7681. [[CrossRef](#)] [[PubMed](#)]
55. Camarero-Espinosa, S.; Rothen-Rutishauser, B.; Foster, E.J.; Weder, C. Articular Cartilage: From Formation to Tissue Engineering. *Biomater. Sci.* **2016**, *4*, 734–767. [[CrossRef](#)] [[PubMed](#)]
56. Decker, R.S.; Koyama, E.; Pacifici, M. Articular Cartilage: Structural and Developmental Intricacies and Questions. *Curr. Osteoporos. Rep.* **2015**, *13*, 407–414. [[CrossRef](#)] [[PubMed](#)]
57. Hunziker, E.B.; Michel, M.; Studer, D. Ultrastructure of Adult Human Articular Cartilage Matrix after Cryotechnical Processing. *Microsc. Res. Tech.* **1997**, *37*, 271–284. [[CrossRef](#)]
58. Egli, P.S.; Hunziker, E.B.; Schenk, R.K. Quantitation of Structural Features Characterizing Weight- and Less-Weight-Bearing Regions in Articular Cartilage: A Stereological Analysis of Medial Femoral Condyles in Young Adult Rabbits. *Anat. Rec.* **1988**, *222*, 217–227. [[CrossRef](#)]

59. Umlauf, D.; Frank, S.; Pap, T.; Bertrand, J. Cartilage Biology, Pathology, and Repair. *Cell Mol. Life Sci.* **2010**, *67*, 4197–4211. [[CrossRef](#)]
60. Redler, I.; Mow, V.C.; Zimny, M.L.; Mansell, J. The Ultrastructure and Biomechanical Significance of the Tidemark of Articular Cartilage. *Clin. Orthop. Relat. Res.* **1975**, *112*, 357–362. [[CrossRef](#)]
61. Mansfield, J.C.; Winlove, C.P. A Multi-Modal Multiphoton Investigation of Microstructure in the Deep Zone and Calcified Cartilage. *J. Anat.* **2012**, *220*, 405–416. [[CrossRef](#)]
62. Youn, I.; Choi, J.B.; Cao, L.; Setton, L.A.; Guilak, F. Zonal Variations in the Three-Dimensional Morphology of the Chondron Measured in Situ Using Confocal Microscopy. *Osteoarthr. Cartil.* **2006**, *14*, 889–897. [[CrossRef](#)]
63. Poole, C.A. Articular Cartilage Chondrons: Form, Function and Failure. *J. Anat.* **1997**, *191 Pt 1*, 1–13. [[CrossRef](#)]
64. Poole, A.R.; Pidoux, I.; Reiner, A.; Rosenberg, L. An Immunoelectron Microscope Study of the Organization of Proteoglycan Monomer, Link Protein, and Collagen in the Matrix of Articular Cartilage. *J. Cell Biol.* **1982**, *93*, 921–937. [[CrossRef](#)]
65. Mansfield, J.C.; Mandalia, V.; Toms, A.; Winlove, C.P.; Brasselet, S. Collagen Reorganization in Cartilage under Strain Probed by Polarization Sensitive Second Harmonic Generation Microscopy. *J. R. Soc. Interface* **2019**, *16*, 20180611. [[CrossRef](#)] [[PubMed](#)]
66. Poole, C.A.; Flint, M.H.; Beaumont, B.W. Chondrons in Cartilage: Ultrastructural Analysis of the Pericellular Microenvironment in Adult Human Articular Cartilages. *J. Orthop. Res.* **1987**, *5*, 509–522. [[CrossRef](#)] [[PubMed](#)]
67. Chandrasekaran, P.; Doyran, B.; Li, Q.; Han, B.; Bechtold, T.E.; Koyama, E.; Lu, X.L.; Han, L. Biomechanical Properties of Murine TMJ Articular Disc and Condyle Cartilage via AFM-Nanoindentation. *J. Biomech.* **2017**, *60*, 134–141. [[CrossRef](#)] [[PubMed](#)]
68. Hunziker, E.B. Articular Cartilage Repair. In *Advances in Osteoarthritis*; Tanaka, S., Hamanishi, C., Eds.; Springer: Tokyo, Japan, 1999; pp. 187–202.
69. Mow, V.C.; Guo, X.E. Mechano-Electrochemical Properties Of Articular Cartilage: Their Inhomogeneities and Anisotropies. *Annu. Rev. Biomed. Eng.* **2002**, *4*, 175–209. [[CrossRef](#)]
70. Brocklehurst, R.; Bayliss, M.T.; Maroudas, A.; Coysh, H.L.; Freeman, M.A.; Revell, P.A.; Ali, S.Y. The Composition of Normal and Osteoarthritic Articular Cartilage from Human Knee Joints. With Special Reference to Unicompartamental Replacement and Osteotomy of the Knee. *J. Bone Jt. Surg. Am.* **1984**, *66*, 95–106. [[CrossRef](#)]
71. Carballo, C.B.; Nakagawa, Y.; Sekiya, I.; Rodeo, S.A. Basic Science of Articular Cartilage. *Clin. Sports Med.* **2017**, *36*, 413–425. [[CrossRef](#)]
72. Roth, V.; Mow, V.C. The Intrinsic Tensile Behavior of the Matrix of Bovine Articular Cartilage and Its Variation with Age. *J. Bone Jt. Surg. Am.* **1980**, *62*, 1102–1117. [[CrossRef](#)]
73. Poole, A.R.; Kojima, T.; Yasuda, T.; Mwale, F.; Kobayashi, M.; Laverty, S. Composition and Structure of Articular Cartilage: A Template for Tissue Repair. *Clin. Orthop. Relat. Res.* **2001**, *391*, S26–S33. [[CrossRef](#)]
74. Woodfield, T.B.F.; Van Blitterswijk, C.A.; De Wijn, J.; Sims, T.J.; Hollander, A.P.; Riesle, J. Polymer Scaffolds Fabricated with Pore-Size Gradients as a Model for Studying the Zonal Organization within Tissue-Engineered Cartilage Constructs. *Tissue Eng.* **2005**, *11*, 1297–1311. [[CrossRef](#)]
75. Schumacher, B.L.; Hughes, C.E.; Kuettner, K.E.; Caterson, B.; Aydelotte, M.B. Immunodetection and Partial cDNA Sequence of the Proteoglycan, Superficial Zone Protein, Synthesized by Cells Lining Synovial Joints. *J. Orthop. Res.* **1999**, *17*, 110–120. [[CrossRef](#)]
76. Warman, M.L. Human Genetic Insights into Skeletal Development, Growth, and Homeostasis. *Clin. Orthop. Relat. Res.* **2000**, *379*, S40–S54. [[CrossRef](#)] [[PubMed](#)]
77. Culav, E.M.; Clark, C.H.; Merrilees, M.J. Connective Tissues: Matrix Composition and Its Relevance to Physical Therapy. *Phys. Ther.* **1999**, *79*, 308–319. [[CrossRef](#)] [[PubMed](#)]
78. Vesentini, S.; Redaelli, A.; Gautieri, A. Nanomechanics of Collagen Microfibrils. *Muscles Ligaments Tendons J.* **2013**, *3*, 23–34. [[CrossRef](#)]
79. Maroudas, A.; Wachtel, E.; Grushko, G.; Katz, E.P.; Weinberg, P. The Effect of Osmotic and Mechanical Pressures on Water Partitioning in Articular Cartilage. *Biochim. Biophys. Acta* **1991**, *1073*, 285–294. [[CrossRef](#)]
80. Torzilli, P.A. Influence of Cartilage Conformation on Its Equilibrium Water Partition. *J. Orthop. Res.* **1985**, *3*, 473–483. [[CrossRef](#)]
81. Lai, W.M.; Hou, J.S.; Mow, V.C. A Triphasic Theory for the Swelling and Deformation Behaviors of Articular Cartilage. *J. Biomech. Eng.* **1991**, *113*, 245–258. [[CrossRef](#)]
82. Buckwalter, J.A.; Mankin, H.J. Articular Cartilage: Tissue Design and Chondrocyte-Matrix Interactions. *Instr. Course Lect.* **1998**, *47*, 477–486. [[PubMed](#)]
83. Nakagawa, Y.; Muneta, T.; Otabe, K.; Ozeki, N.; Mizuno, M.; Udo, M.; Saito, R.; Yanagisawa, K.; Ichinose, S.; Koga, H.; et al. Cartilage Derived from Bone Marrow Mesenchymal Stem Cells Expresses Lubricin In Vitro and In Vivo. *PLoS ONE* **2016**, *11*, e0148777. [[CrossRef](#)] [[PubMed](#)]
84. Ateshian, G.A.; Warden, W.H.; Kim, J.J.; Grelsamer, R.P.; Mow, V.C. Finite Deformation Biphasic Material Properties of Bovine Articular Cartilage from Confined Compression Experiments. *J. Biomech.* **1997**, *30*, 1157–1164. [[CrossRef](#)]
85. Frank, E.H.; Grodzinsky, A.J. Cartilage Electromechanics—I. Electrokinetic Transduction and the Effects of Electrolyte pH and Ionic Strength. *J. Biomech.* **1987**, *20*, 615–627. [[CrossRef](#)]
86. Schmidt, T.A.; Gastelum, N.S.; Nguyen, Q.T.; Schumacher, B.L.; Sah, R.L. Boundary Lubrication of Articular Cartilage: Role of Synovial Fluid Constituents. *Arthritis Rheum.* **2007**, *56*, 882–891. [[CrossRef](#)] [[PubMed](#)]
87. Daniel, M. Boundary Cartilage Lubrication: Review of Current Concepts. *Wien. Med. Wochenschr.* **2014**, *164*, 88–94. [[CrossRef](#)]

88. Mattson, J.M.; Turcotte, R.; Zhang, Y. Glycosaminoglycans Contribute to Extracellular Matrix Fiber Recruitment and Arterial Wall Mechanics. *Biomech. Model. Mechanobiol.* **2017**, *16*, 213–225. [[CrossRef](#)]
89. Brody, L.T. Knee Osteoarthritis: Clinical Connections to Articular Cartilage Structure and Function. *Phys. Ther. Sport.* **2015**, *16*, 301–316. [[CrossRef](#)]
90. Whitesides, T. Orthopaedic Basic Science. Biology and Biomechanics of the Musculoskeletal System. 2nd ed. *J. Bone Jt. Surg.-Am. Vol.* **2001**, *83*, 482. [[CrossRef](#)]
91. Moutos, F.T.; Freed, L.E.; Guilak, F. A Biomimetic Three-Dimensional Woven Composite Scaffold for Functional Tissue Engineering of Cartilage. *Nat. Mater.* **2007**, *6*, 162–167. [[CrossRef](#)]
92. Ateshian, G.A. The Role of Interstitial Fluid Pressurization in Articular Cartilage Lubrication. *J. Biomech.* **2009**, *42*, 1163–1176. [[CrossRef](#)]
93. Cohen, N.P.; Foster, R.J.; Mow, V.C. Composition and Dynamics of Articular Cartilage: Structure, Function, and Maintaining Healthy State. *J. Orthop. Sports Phys. Ther.* **1998**, *28*, 203–215. [[CrossRef](#)] [[PubMed](#)]
94. Mow, V.C.; Holmes, M.H.; Lai, W.M. Fluid Transport and Mechanical Properties of Articular Cartilage: A Review. *J. Biomech.* **1984**, *17*, 377–394. [[CrossRef](#)]
95. Soltz, M.A.; Ateshian, G.A. Experimental Verification and Theoretical Prediction of Cartilage Interstitial Fluid Pressurization at an Impermeable Contact Interface in Confined Compression. *J. Biomech.* **1998**, *31*, 927–934. [[CrossRef](#)] [[PubMed](#)]
96. Park, S.; Ateshian, G. Dynamic Response of Immature Bovine Articular Cartilage in Tension and Compression, and Nonlinear Viscoelastic Modeling of the Tensile Response. *J. Biomech. Eng.* **2006**, *128*, 623–630. [[CrossRef](#)] [[PubMed](#)]
97. Maroudas, A. Fluid Transport in Cartilage. *Ann. Rheum. Dis.* **1975**, *34* (Suppl. S2), S77–S81.
98. Maroudas, A. Biophysical Chemistry of Cartilaginous Tissues with Special Reference to Solute and Fluid Transport. *Biorheology* **1975**, *12*, 233–248. [[CrossRef](#)]
99. Mansour, J.M.; Mow, V.C. The Permeability of Articular Cartilage under Compressive Strain and at High Pressures. *J. Bone Jt. Surg. Am.* **1976**, *58*, 509–516. [[CrossRef](#)]
100. Armstrong, C.G.; Mow, V.C. Variations in the Intrinsic Mechanical Properties of Human Articular Cartilage with Age, Degeneration, and Water Content. *J. Bone Jt. Surg. Am.* **1982**, *64*, 88–94. [[CrossRef](#)]
101. Mow, V.C.; Kuei, S.C.; Lai, W.M.; Armstrong, C.G. Biphasic Creep and Stress Relaxation of Articular Cartilage in Compression: Theory and Experiments. *J. Biomech. Eng.* **1980**, *102*, 73–84. [[CrossRef](#)]
102. Mak, A.F.; Lai, W.M.; Mow, V.C. Biphasic Indentation of Articular Cartilage—I. Theoretical Analysis. *J. Biomech.* **1987**, *20*, 703–714. [[CrossRef](#)]
103. Katta, J.; Jin, Z.; Ingham, E.; Fisher, J. Biotribology of Articular Cartilage—A Review of the Recent Advances. *Med. Eng. Phys.* **2008**, *30*, 1349–1363. [[CrossRef](#)] [[PubMed](#)]
104. Grushko, G.; Schneiderman, R.; Maroudas, A. Some Biochemical and Biophysical Parameters for the Study of the Pathogenesis of Osteoarthritis: A Comparison between the Processes of Ageing and Degeneration in Human Hip Cartilage. *Connect. Tissue Res.* **1989**, *19*, 149–176. [[CrossRef](#)] [[PubMed](#)]
105. Afoke, N.Y.; Byers, P.D.; Hutton, W.C. Contact Pressures in the Human Hip Joint. *J. Bone Jt. Surg. Br.* **1987**, *69*, 536–541. [[CrossRef](#)] [[PubMed](#)]
106. Whitaker, S. Flow in Porous Media I: A Theoretical Derivation of Darcy's Law. *Transp. Porous Med.* **1986**, *1*, 3–25. [[CrossRef](#)]
107. Leaf, A. Maintenance of concentration gradients and regulation of cell volume. *Ann. N. Y. Acad. Sci.* **1959**, *72*, 396–404. [[CrossRef](#)] [[PubMed](#)]
108. Teeple, E.; Fleming, B.C.; Mechrefe, A.P.; Crisco, J.J.; Brady, M.F.; Jay, G.D. Frictional Properties of Hartley Guinea Pig Knees with and without Proteolytic Disruption of the Articular Surfaces. *Osteoarthr. Cartil.* **2007**, *15*, 309–315. [[CrossRef](#)] [[PubMed](#)]
109. Armstrong, C.G.; Bahrani, A.S.; Gardner, D.L. In vitro measurement of articular cartilage deformations in the intact human hip joint under load. *J. Bone Jt. Surg. Br. Vol.* **1979**, *61*, 744–755. [[CrossRef](#)]
110. Zhu, W.; Mow, V.C.; Koob, T.J.; Eyre, D.R. Viscoelastic Shear Properties of Articular Cartilage and the Effects of Glycosidase Treatments. *J. Orthop. Res.* **1993**, *11*, 771–781. [[CrossRef](#)]
111. Wong, B.L.; Sah, R.L. Mechanical Asymmetry during Articulation of Tibial and Femoral Cartilages: Local and Overall Compressive and Shear Deformation and Properties. *J. Biomech.* **2010**, *43*, 1689–1695. [[CrossRef](#)] [[PubMed](#)]
112. Huttu, M.R.J.; Puhakka, J.; Mäkelä, J.T.A.; Takakubo, Y.; Tiitu, V.; Saarakkala, S.; Kontinen, Y.T.; Kiviranta, I.; Korhonen, R.K. Cell-Tissue Interactions in Osteoarthritic Human Hip Joint Articular Cartilage. *Connect. Tissue Res.* **2014**, *55*, 282–291. [[CrossRef](#)]
113. Nissinen, M.T.; Hänninen, N.; Prakash, M.; Mäkelä, J.T.A.; Nissi, M.J.; Töyräs, J.; Nieminen, M.T.; Korhonen, R.K.; Tanska, P. Functional and Structural Properties of Human Patellar Articular Cartilage in Osteoarthritis. *J. Biomech.* **2021**, *126*, 110634. [[CrossRef](#)] [[PubMed](#)]
114. Inhatouski, M.; Pauk, J.; Karev, D.; Karev, B. AFM-Based Method for Measurement of Normal and Osteoarthritic Human Articular Cartilage Surface Roughness. *Materials* **2020**, *13*, 2302. [[CrossRef](#)] [[PubMed](#)]
115. Fischenich, K.M.; Wahlquist, J.A.; Wilmoth, R.L.; Cai, L.; Neu, C.P.; Ferguson, V.L. Human Articular Cartilage Is Orthotropic Where Microstructure, Micromechanics, and Chemistry Vary with Depth and Split-Line Orientation. *Osteoarthr. Cartil.* **2020**, *28*, 1362–1372. [[CrossRef](#)] [[PubMed](#)]
116. Link, J.M.; Salinas, E.Y.; Hu, J.C.; Athanasiou, K.A. The Tribology of Cartilage: Mechanisms, Experimental Techniques, and Relevance to Translational Tissue Engineering. *Clin. Biomech.* **2020**, *79*, 104880. [[CrossRef](#)] [[PubMed](#)]

117. Moore, A.C.; Burris, D.L. Tribological and Material Properties for Cartilage of and throughout the Bovine Stifle: Support for the Altered Joint Kinematics Hypothesis of Osteoarthritis. *Osteoarthr. Cartil.* **2015**, *23*, 161–169. [[CrossRef](#)] [[PubMed](#)]
118. Forster, H.; Fisher, J. The Influence of Continuous Sliding and Subsequent Surface Wear on the Friction of Articular Cartilage. *Proc. Inst. Mech. Eng. H.* **1999**, *213*, 329–345. [[CrossRef](#)] [[PubMed](#)]
119. McCutchen, C.W. The Frictional Properties of Animal Joints. *Wear* **1962**, *5*, 1–17. [[CrossRef](#)]
120. Mostakhdemin, M.; Nand, A.; Ramezani, M. Articular and Artificial Cartilage, Characteristics, Properties and Testing Approaches—A Review. *Polymers* **2021**, *13*, 2000. [[CrossRef](#)] [[PubMed](#)]
121. Kienle, S.; Boettcher, K.; Wiegler, L.; Urban, J.; Burgkart, R.; Lieleg, O.; Hugel, T. Comparison of Friction and Wear of Articular Cartilage on Different Length Scales. *J. Biomech.* **2015**, *48*, 3052–3058. [[CrossRef](#)]
122. Hossain, M.J.; Noori-Dokht, H.; Karnik, S.; Alyafei, N.; Joukar, A.; Trippel, S.B.; Wagner, D.R. Anisotropic Properties of Articular Cartilage in an Accelerated in Vitro Wear Test. *J. Mech. Behav. Biomed. Mater.* **2020**, *109*, 103834. [[CrossRef](#)]
123. Middendorf, J.M.; Griffin, D.J.; Shortkroff, S.; Dugopolski, C.; Kennedy, S.; Siemiatkoski, J.; Cohen, I.; Bonassar, L.J. Mechanical Properties and Structure-Function Relationships of Human Chondrocyte-Seeded Cartilage Constructs after in Vitro Culture. *J. Orthop. Res.* **2017**, *35*, 2298–2306. [[CrossRef](#)] [[PubMed](#)]
124. Li, F.; Su, Y.; Wang, J.; Wu, G.; Wang, C. Influence of Dynamic Load on Friction Behavior of Human Articular Cartilage, Stainless Steel and Polyvinyl Alcohol Hydrogel as Artificial Cartilage. *J. Mater. Sci: Mater. Med.* **2010**, *21*, 147–154. [[CrossRef](#)] [[PubMed](#)]
125. Li, F.; Wang, A.; Wang, C. Analysis of Friction between Articular Cartilage and Polyvinyl Alcohol Hydrogel Artificial Cartilage. *J. Mater. Sci: Mater. Med.* **2016**, *27*, 87. [[CrossRef](#)] [[PubMed](#)]
126. Little, C.J.; Bawolin, N.K.; Chen, X. Mechanical Properties of Natural Cartilage and Tissue-Engineered Constructs. *Tissue Eng. Part B Rev.* **2011**, *17*, 213–227. [[CrossRef](#)] [[PubMed](#)]
127. Hlaváček, M. The Thixotropic Effect of the Synovial Fluid in Squeeze-Film Lubrication of the Human Hip Joint. *Biorheology* **2001**, *38*, 319–334. [[PubMed](#)]
128. He, B.; Wang, C.; Xiong, X.; Li, J.; Jin, Z.; Qu, S. Bio-inspired Low Wear and Durable Lubrication Interfacial System Based on Thixotropic Hydrogel for Artificial Joints. *Biosurface Biotribology* **2023**, *9*, 59–70. [[CrossRef](#)]
129. Hlaváček, M. The Influence of the Acetabular Labrum Seal, Intact Articular Superficial Zone and Synovial Fluid Thixotropy on Squeeze-Film Lubrication of a Spherical Synovial Joint. *J. Biomech.* **2002**, *35*, 1325–1335. [[CrossRef](#)] [[PubMed](#)]
130. Wright, V.; Dowson, D. Lubrication and Cartilage. *J. Anat.* **1976**, *121*, 107–118.
131. Amarouch, M.Y.; El Hilaly, J.; Mazouzi, D. AFM and FluidFM Technologies: Recent Applications in Molecular and Cellular Biology. *Scanning* **2018**, *2018*, 7801274. [[CrossRef](#)]
132. Desrochers, J.; Amrein, M.W.; Matyas, J.R. Microscale Surface Friction of Articular Cartilage in Early Osteoarthritis. *J. Mech. Behav. Biomed. Mater.* **2013**, *25*, 11–22. [[CrossRef](#)]
133. Braet; Seynaeve; Zanger, D.; Wisse. Imaging Surface and Submembranous Structures with the Atomic Force Microscope: A Study on Living Cancer Cells, Fibroblasts and Macrophages. *J. Microsc.* **1998**, *190*, 328–338. [[CrossRef](#)] [[PubMed](#)]
134. Peters, A.E.; Akhtar, R.; Comerford, E.J.; Bates, K.T. The Effect of Ageing and Osteoarthritis on the Mechanical Properties of Cartilage and Bone in the Human Knee Joint. *Sci. Rep.* **2018**, *8*, 5931. [[CrossRef](#)] [[PubMed](#)]
135. Seidenstuecker, M.; Watrinet, J.; Bernstein, A.; Suedkamp, N.P.; Latorre, S.H.; Maks, A.; Mayr, H.O. Viscoelasticity and Histology of the Human Cartilage in Healthy and Degenerated Conditions of the Knee. *J. Orthop. Surg. Res.* **2019**, *14*, 256. [[CrossRef](#)] [[PubMed](#)]
136. Dourthe, B.; Nickmanesh, R.; Wilson, D.R.; D’Agostino, P.; Patwa, A.N.; Grinstaff, M.W.; Snyder, B.D.; Vereecke, E. Assessment of Healthy Trapeziometacarpal Cartilage Properties Using Indentation Testing and Contrast-Enhanced Computed Tomography. *Clin. Biomech.* **2019**, *61*, 181–189. [[CrossRef](#)] [[PubMed](#)]
137. Zimmerman, B.K.; Nims, R.J.; Chen, A.; Hung, C.T.; Ateshian, G.A. Direct Osmotic Pressure Measurements in Articular Cartilage Demonstrate Nonideal and Concentration-Dependent Phenomena. *J. Biomech. Eng.* **2021**, *143*, 041007. [[CrossRef](#)] [[PubMed](#)]
138. Kleemann, R.U.; Krocker, D.; Cedraro, A.; Tuischer, J.; Duda, G.N. Altered Cartilage Mechanics and Histology in Knee Osteoarthritis: Relation to Clinical Assessment (ICRS Grade). *Osteoarthr. Cartil.* **2005**, *13*, 958–963. [[CrossRef](#)] [[PubMed](#)]
139. Boschetti, F.; Peretti, G.M. Tensile and Compressive Properties of Healthy and Osteoarthritic Human Articular Cartilage. *Biorheology* **2008**, *45*, 337–344. [[CrossRef](#)] [[PubMed](#)]
140. Mäkelä, J.T.A.; Huttu, M.R.J.; Korhonen, R.K. Structure–Function Relationships in Osteoarthritic Human Hip Joint Articular Cartilage. *Osteoarthr. Cartil.* **2012**, *20*, 1268–1277. [[CrossRef](#)] [[PubMed](#)]
141. Kempson, G.E. Age-Related Changes in the Tensile Properties of Human Articular Cartilage: A Comparative Study between the Femoral Head of the Hip Joint and the Talus of the Ankle Joint. *Biochim. Biophys. Acta (BBA)-Gen. Subj.* **1991**, *1075*, 223–230. [[CrossRef](#)]
142. Temple-Wong, M.M.; Bae, W.C.; Chen, M.Q.; Bugbee, W.D.; Amiel, D.; Coutts, R.D.; Lotz, M.; Sah, R.L. Biomechanical, Structural, and Biochemical Indices of Degenerative and Osteoarthritic Deterioration of Adult Human Articular Cartilage of the Femoral Condyle. *Osteoarthr. Cartil.* **2009**, *17*, 1469–1476. [[CrossRef](#)]
143. Berardo, A.; Costagliola, G.; Ghio, S.; Boscardin, M.; Bosia, F.; Pugno, N.M. An Experimental-Numerical Study of the Adhesive Static and Dynamic Friction of Micro-Patterned Soft Polymer Surfaces. *Mater. Des.* **2019**, *181*, 107930. [[CrossRef](#)]
144. Berardo, A.; Pugno, N.M. A Model for Hierarchical Anisotropic Friction, Adhesion and Wear. *Tribol. Int.* **2020**, *152*, 106549. [[CrossRef](#)]

145. Spagni, A.; Berardo, A.; Marchetto, D.; Gualtieri, E.; Pugno, N.M.; Valeri, S. Friction of Rough Surfaces on Ice: Experiments and Modeling. *Wear* **2016**, *368–369*, 258–266. [[CrossRef](#)]
146. Lakin, B.A.; Grasso, D.J.; Shah, S.S.; Stewart, R.C.; Bansal, P.N.; Freedman, J.D.; Grinstaff, M.W.; Snyder, B.D. Cationic Agent Contrast-Enhanced Computed Tomography Imaging of Cartilage Correlates with the Compressive Modulus and Coefficient of Friction. *Osteoarthr. Cartil.* **2013**, *21*, 60–68. [[CrossRef](#)] [[PubMed](#)]
147. Krishnan, R.; Kopacz, M.; Ateshian, G.A. Experimental Verification of the Role of Interstitial Fluid Pressurization in Cartilage Lubrication. *J. Orthop. Res.* **2004**, *22*, 565–570. [[CrossRef](#)] [[PubMed](#)]
148. Katta, J.; Stapleton, T.; Ingham, E.; Jin, Z.M.; Fisher, J. The Effect of Glycosaminoglycan Depletion on the Friction and Deformation of Articular Cartilage. *Proc. Inst. Mech. Eng. H.* **2008**, *222*, 1–11. [[CrossRef](#)] [[PubMed](#)]
149. Forster, H.; Fisher, J. The Influence of Loading Time and Lubricant on the Friction of Articular Cartilage. *Proc. Inst. Mech. Eng. H.* **1996**, *210*, 109–119. [[CrossRef](#)] [[PubMed](#)]
150. Zimmerman, B.K.; Bonnevie, E.D.; Park, M.; Zhou, Y.; Wang, L.; Burris, D.L.; Lu, X.L. Role of Interstitial Fluid Pressurization in TMJ Lubrication. *J. Dent. Res.* **2015**, *94*, 85–92. [[CrossRef](#)] [[PubMed](#)]
151. Caligaris, M.; Ateshian, G.A. Effects of Sustained Interstitial Fluid Pressurization under Migrating Contact Area, and Boundary Lubrication by Synovial Fluid, on Cartilage Friction. *Osteoarthr. Cartil.* **2008**, *16*, 1220–1227. [[CrossRef](#)]
152. Musumeci, G.; Aiello, F.; Szychlińska, M.; Di Rosa, M.; Castrogiovanni, P.; Mobasher, A. Osteoarthritis in the XXIst Century: Risk Factors and Behaviours That Influence Disease Onset and Progression. *IJMS* **2015**, *16*, 6093–6112. [[CrossRef](#)]
153. Mobasher, A.; Batt, M. An Update on the Pathophysiology of Osteoarthritis. *Ann. Phys. Rehabil. Med.* **2016**, *59*, 333–339. [[CrossRef](#)]
154. McKenna, C.H.; Hunder, G.G. Arthritis and Allied Conditions: A Textbook of Rheumatology. *Arthritis Rheum.* **1973**, *16*, 528–529. [[CrossRef](#)]
155. Roberts, S.; Weightman, B.; Urban, J.; Chappell, D. Mechanical and Biochemical Properties of Human Articular Cartilage in Osteoarthritic Femoral Heads and in Autopsy Specimens. *J. Bone Jt. Surgery. Br. Vol.* **1986**, *68-B*, 278–288. [[CrossRef](#)]
156. Calvo, E.; Palacios, I.; Delgado, E.; Sánchez-Pernaute, O.; Largo, R.; Egido, J.; Herrero-Beaumont, G. Histopathological Correlation of Cartilage Swelling Detected by Magnetic Resonance Imaging in Early Experimental Osteoarthritis. *Osteoarthr. Cartil.* **2004**, *12*, 878–886. [[CrossRef](#)]
157. Akizuki, S.; Mow, V.C.; Muller, F.; Pita, J.C.; Howell, D.S. Tensile Properties of Human Knee Joint Cartilage. II. Correlations between Weight Bearing and Tissue Pathology and the Kinetics of Swelling. *J. Orthop. Res.* **1987**, *5*, 173–186. [[CrossRef](#)] [[PubMed](#)]
158. Wu, W.; Billingham, R.C.; Pidoux, I.; Antoniou, J.; Zukor, D.; Tanzer, M.; Poole, A.R. Sites of Collagenase Cleavage and Denaturation of Type II Collagen in Aging and Osteoarthritic Articular Cartilage and Their Relationship to the Distribution of Matrix Metalloproteinase 1 and Matrix Metalloproteinase 13. *Arthritis Rheum.* **2002**, *46*, 2087–2094. [[CrossRef](#)] [[PubMed](#)]
159. Radin, E.L.; Burr, D.B.; Caterson, B.; Fyhrie, D.; Brown, T.D.; Boyd, R.D. Mechanical Determinants of Osteoarthrosis. *Semin. Arthritis Rheum.* **1991**, *21*, 12–21. [[CrossRef](#)] [[PubMed](#)]
160. Stannus, O.; Jones, G.; Cicuttini, F.; Parameswaran, V.; Quinn, S.; Burgess, J.; Ding, C. Circulating Levels of IL-6 and TNF- α Are Associated with Knee Radiographic Osteoarthritis and Knee Cartilage Loss in Older Adults. *Osteoarthr. Cartil.* **2010**, *18*, 1441–1447. [[CrossRef](#)]
161. Malemud, C.J. Anticytokine Therapy for Osteoarthritis: Evidence to Date. *Drugs Aging* **2010**, *27*, 95–115. [[CrossRef](#)]
162. Liacini, A. Induction of Matrix Metalloproteinase-13 Gene Expression by TNF- α Is Mediated by MAP Kinases, AP-1, and NF- κ B Transcription Factors in Articular Chondrocytes. *Exp. Cell Res.* **2003**, *288*, 208–217. [[CrossRef](#)]
163. Chery, D.R.; Han, B.; Li, Q.; Zhou, Y.; Heo, S.-J.; Kwok, B.; Chandrasekaran, P.; Wang, C.; Qin, L.; Lu, X.L.; et al. Early Changes in Cartilage Pericellular Matrix Micromechanobiology Portend the Onset of Post-Traumatic Osteoarthritis. *Acta Biomater.* **2020**, *111*, 267–278. [[CrossRef](#)] [[PubMed](#)]
164. Mehana, E.-S.E.; Khafaga, A.F.; El-Blehi, S.S. The Role of Matrix Metalloproteinases in Osteoarthritis Pathogenesis: An Updated Review. *Life Sci.* **2019**, *234*, 116786. [[CrossRef](#)] [[PubMed](#)]
165. Ruthard, J.; Hermes, G.; Hartmann, U.; Sengle, G.; Pongratz, G.; Ostendorf, B.; Schneider, M.; Höllriegel, S.; Zaucke, F.; Wagener, R.; et al. Identification of Antibodies against Extracellular Matrix Proteins in Human Osteoarthritis. *Biochem. Biophys. Res. Commun.* **2018**, *503*, 1273–1277. [[CrossRef](#)] [[PubMed](#)]
166. Bersellini Farinotti, A.; Wigerblad, G.; Nascimento, D.; Bas, D.B.; Morado Urbina, C.; Nandakumar, K.S.; Sandor, K.; Xu, B.; Abdelmoaty, S.; Hunt, M.A.; et al. Cartilage-Binding Antibodies Induce Pain through Immune Complex-Mediated Activation of Neurons. *J. Exp. Med.* **2019**, *216*, 1904–1924. [[CrossRef](#)] [[PubMed](#)]
167. Hu, Y.; Chen, X.; Wang, S.; Jing, Y.; Su, J. Subchondral Bone Microenvironment in Osteoarthritis and Pain. *Bone Res.* **2021**, *9*, 20. [[CrossRef](#)] [[PubMed](#)]
168. Xie, H.; Cui, Z.; Wang, L.; Xia, Z.; Hu, Y.; Xian, L.; Li, C.; Xie, L.; Crane, J.; Wan, M.; et al. PDGF-BB Secreted by Preosteoclasts Induces Angiogenesis during Coupling with Osteogenesis. *Nat. Med.* **2014**, *20*, 1270–1278. [[CrossRef](#)] [[PubMed](#)]
169. Tu, M.; Yang, M.; Yu, N.; Zhen, G.; Wan, M.; Liu, W.; Ji, B.; Ma, H.; Guo, Q.; Tong, P.; et al. Inhibition of Cyclooxygenase-2 Activity in Subchondral Bone Modifies a Subtype of Osteoarthritis. *Bone Res.* **2019**, *7*, 29. [[CrossRef](#)] [[PubMed](#)]
170. Zhou, S.; Thornhill, T.S.; Meng, F.; Xie, L.; Wright, J.; Glowacki, J. Influence of Osteoarthritis Grade on Molecular Signature of Human Cartilage: OSTEOARTHRITIS AND GENE EXPRESSION. *J. Orthop. Res.* **2016**, *34*, 454–462. [[CrossRef](#)]

171. Pritzker, K.P.H.; Gay, S.; Jimenez, S.A.; Ostergaard, K.; Pelletier, J.-P.; Revell, P.A.; Salter, D.; Van Den Berg, W.B. Osteoarthritis Cartilage Histopathology: Grading and Staging. *Osteoarthr. Cartil.* **2006**, *14*, 13–29. [[CrossRef](#)]
172. Sokoloff, L. The Biology of Degenerative Joint Disease. *Acta Rheumatol. Belg.* **1977**, *1*, 155–156. [[CrossRef](#)]
173. van den Borne, M.P.J.; Raijmakers, N.J.H.; Vanlauwe, J.; Victor, J.; de Jong, S.N.; Bellemans, J.; Saris, D.B.F. International Cartilage Repair Society (ICRS) and Oswestry Macroscopic Cartilage Evaluation Scores Validated for Use in Autologous Chondrocyte Implantation (ACI) and Microfracture. *Osteoarthr. Cartil.* **2007**, *15*, 1397–1402. [[CrossRef](#)] [[PubMed](#)]
174. Burr, D.B.; Gallant, M.A. Bone Remodelling in Osteoarthritis. *Nat. Rev. Rheumatol.* **2012**, *8*, 665–673. [[CrossRef](#)] [[PubMed](#)]
175. Raynauld, J.-P.; Martel-Pelletier, J.; Berthiaume, M.-J.; Abram, F.; Choquette, D.; Haraoui, B.; Beary, J.F.; Cline, G.A.; Meyer, J.M.; Pelletier, J.-P. Correlation between Bone Lesion Changes and Cartilage Volume Loss in Patients with Osteoarthritis of the Knee as Assessed by Quantitative Magnetic Resonance Imaging over a 24-Month Period. *Ann. Rheum. Dis.* **2007**, *67*, 683–688. [[CrossRef](#)] [[PubMed](#)]
176. Goldring, S.R. Role of Bone in Osteoarthritis Pathogenesis. *Med. Clin. N. Am.* **2009**, *93*, 25–35. [[CrossRef](#)] [[PubMed](#)]
177. Crema, M.D.; Roemer, F.W.; Zhu, Y.; Marra, M.D.; Niu, J.; Zhang, Y.; Lynch, J.A.; Javaid, M.K.; Lewis, C.E.; El-Khoury, G.Y.; et al. Subchondral Cystlike Lesions Develop Longitudinally in Areas of Bone Marrow Edema-like Lesions in Patients with or at Risk for Knee Osteoarthritis: Detection with MR Imaging—The MOST Study. *Radiology* **2010**, *256*, 855–862. [[CrossRef](#)] [[PubMed](#)]
178. Pottenger, L.A.; Phillips, F.M.; Draganich, L.F. The Effect of Marginal Osteophytes on Reduction of Varus-Valgus Instability in Osteoarthritic Knees. *Arthritis Rheum.* **1990**, *33*, 853–858. [[CrossRef](#)] [[PubMed](#)]
179. Felson, D.T. Osteophytes and Progression of Knee Osteoarthritis. *Rheumatology* **2005**, *44*, 100–104. [[CrossRef](#)] [[PubMed](#)]
180. Scanzello, C.R.; Goldring, S.R. The Role of Synovitis in Osteoarthritis Pathogenesis. *Bone* **2012**, *51*, 249–257. [[CrossRef](#)] [[PubMed](#)]
181. Schumacher, B.L.; Block, J.A.; Schmid, T.M.; Aydelotte, M.B.; Kuettner, K.E. A Novel Proteoglycan Synthesized and Secreted by Chondrocytes of the Superficial Zone of Articular Cartilage. *Arch. Biochem. Biophys.* **1994**, *311*, 144–152. [[CrossRef](#)]
182. Jay, G.D.; Britt, D.E.; Cha, C.J. Lubricin Is a Product of Megakaryocyte Stimulating Factor Gene Expression by Human Synovial Fibroblasts. *J. Rheumatol.* **2000**, *27*, 594–600.
183. Swann, D.A.; Silver, F.H.; Slayter, H.S.; Stafford, W.; Shore, E. The Molecular Structure and Lubricating Activity of Lubricin Isolated from Bovine and Human Synovial Fluids. *Biochem. J.* **1985**, *225*, 195–201. [[CrossRef](#)]
184. Bastow, E.R.; Byers, S.; Golub, S.B.; Clarkin, C.E.; Pitsillides, A.A.; Fosang, A.J. Hyaluronan Synthesis and Degradation in Cartilage and Bone. *Cell. Mol. Life Sci.* **2008**, *65*, 395–413. [[CrossRef](#)]
185. Ludwig, T.E.; McAllister, J.R.; Lun, V.; Wiley, J.P.; Schmidt, T.A. Diminished Cartilage-Lubricating Ability of Human Osteoarthritic Synovial Fluid Deficient in Proteoglycan 4: Restoration through Proteoglycan 4 Supplementation. *Arthritis Rheum.* **2012**, *64*, 3963–3971. [[CrossRef](#)]
186. Kosinska, M.K.; Ludwig, T.E.; Liebisch, G.; Zhang, R.; Siebert, H.-C.; Wilhelm, J.; Kaesser, U.; Dettmeyer, R.B.; Klein, H.; Ishaque, B.; et al. Articular Joint Lubricants during Osteoarthritis and Rheumatoid Arthritis Display Altered Levels and Molecular Species. *PLoS ONE* **2015**, *10*, e0125192. [[CrossRef](#)] [[PubMed](#)]
187. Schmidt, T.A.; Sah, R.L. Effect of Synovial Fluid on Boundary Lubrication of Articular Cartilage. *Osteoarthr. Cartil.* **2007**, *15*, 35–47. [[CrossRef](#)]
188. Jay, G.D.; Elsaid, K.A.; Zack, J.; Robinson, K.; Trespalacios, F.; Cha, C.-J.; Chichester, C.O. Lubricating Ability of Aspirated Synovial Fluid from Emergency Department Patients with Knee Joint Synovitis. *J. Rheumatol.* **2004**, *31*, 557–564.
189. Elsaid, K.A.; Chichester, C.O. Review: Collagen Markers in Early Arthritic Diseases. *Clin. Chim. Acta* **2006**, *365*, 68–77. [[CrossRef](#)] [[PubMed](#)]
190. Young, A.; McLennan, S.; Smith, M.; Smith, S.; Cake, M.; Read, R.; Melrose, J.; Sonnabend, D.; Flannery, C.; Little, C. Proteoglycan 4 Downregulation in a Sheep Meniscectomy Model of Early Osteoarthritis. *Arthritis Res. Ther.* **2006**, *8*, R41. [[CrossRef](#)]
191. Elsaid, K.A.; Jay, G.D.; Warman, M.L.; Rhee, D.K.; Chichester, C.O. Association of Articular Cartilage Degradation and Loss of Boundary-Lubricating Ability of Synovial Fluid Following Injury and Inflammatory Arthritis. *Arthritis Rheum.* **2005**, *52*, 1746–1755. [[CrossRef](#)]
192. Teeple, E.; Elsaid, K.A.; Fleming, B.C.; Jay, G.D.; Aslani, K.; Crisco, J.J.; Mechrefe, A.P. Coefficients of Friction, Lubricin, and Cartilage Damage in the Anterior Cruciate Ligament-Deficient Guinea Pig Knee. *J. Orthop. Res.* **2008**, *26*, 231–237. [[CrossRef](#)] [[PubMed](#)]
193. Rhee, D.K.; Marcelino, J.; Baker, M.; Gong, Y.; Smits, P.; Lefebvre, V.; Jay, G.D.; Stewart, M.; Wang, H.; Warman, M.L.; et al. The Secreted Glycoprotein Lubricin Protects Cartilage Surfaces and Inhibits Synovial Cell Overgrowth. *J. Clin. Investig.* **2005**, *115*, 622–631. [[CrossRef](#)] [[PubMed](#)]
194. Waller, K.A.; Zhang, L.X.; Elsaid, K.A.; Fleming, B.C.; Warman, M.L.; Jay, G.D. Role of Lubricin and Boundary Lubrication in the Prevention of Chondrocyte Apoptosis. *Proc. Natl. Acad. Sci. USA* **2013**, *110*, 5852–5857. [[CrossRef](#)]
195. Kempson, G.E.; Freeman, M.A.R.; Swanson, S.A.V. Tensile Properties of Articular Cartilage. *Nature* **1968**, *220*, 1127–1128. [[CrossRef](#)]
196. Woo, S.L.-Y.; Akeson, W.H.; Jemmott, G.F. Measurements of Nonhomogeneous, Directional Mechanical Properties of Articular Cartilage in Tension. *J. Biomech.* **1976**, *9*, 785–791. [[CrossRef](#)] [[PubMed](#)]
197. Kempson, G.; Muir, H.; Pollard, C.; Tuke, M. The Tensile Properties of the Cartilage of Human Femoral Condyles Related to the Content of Collagen and Glycosaminoglycans. *Biochim. Biophys. Acta (BBA)-Gen. Subj.* **1973**, *297*, 456–472. [[CrossRef](#)]

198. Akizuki, S.; Mow, V.C.; Müller, F.; Pita, J.C.; Howell, D.S.; Manicourt, D.H. Tensile Properties of Human Knee Joint Cartilage: I. Influence of Ionic Conditions, Weight Bearing, and Fibrillation on the Tensile Modulus: Tensile Modulus of Human Knee Cartilage. *J. Orthop. Res.* **1986**, *4*, 379–392. [[CrossRef](#)]
199. Hayes, W.C.; Mockros, L.F. Viscoelastic Properties of Human Articular Cartilage. *J. Appl. Physiol.* **1971**, *31*, 562–568. [[CrossRef](#)]
200. Sokoloff, L. Elasticity of Aging Cartilage. *Fed. Proc.* **1966**, *25*, 1089–1095.
201. Ding, M.; Dalstra, M.; Linde, F.; Hvid, I. Changes in the Stiffness of the Human Tibial Cartilage-Bone Complex in Early-Stage Osteoarthritis. *Acta Orthop. Scand.* **1998**, *69*, 358–362. [[CrossRef](#)]
202. Rivers, P.A.; Rosenwasser, M.P.; Mow, V.C.; Pawluk, R.J.; Strauch, R.J.; Sugalski, M.T.; Ateshian, G.A. Osteoarthritic Changes in the Biochemical Composition of Thumb Carpometacarpal Joint Cartilage and Correlation with Biomechanical Properties. *J. Hand Surg.* **2000**, *25*, 889–898. [[CrossRef](#)]
203. Gu, W.Y.; Lai, W.M.; Mow, V.C. Transport of Fluid and Ions through a Porous-Permeable Charged-Hydrated Tissue, and Streaming Potential Data on Normal Bovine Articular Cartilage. *J. Biomech.* **1993**, *26*, 709–723. [[CrossRef](#)]
204. Ebrahimi, M.; Ojanen, S.; Mohammadi, A.; Finnilä, M.A.; Joukainen, A.; Kröger, H.; Saarakkala, S.; Korhonen, R.K.; Tanska, P. Elastic, Viscoelastic and Fibril-Reinforced Poroelastic Material Properties of Healthy and Osteoarthritic Human Tibial Cartilage. *Ann. Biomed. Eng.* **2019**, *47*, 953–966. [[CrossRef](#)]
205. Brittberg, M.; Lindahl, A.; Nilsson, A. Treatment of Deep Cartilage Defects in the Knee with Autologous Chondrocyte Transplantation. *N. Engl. J. Med.* **1994**, *331*, 889–895. [[CrossRef](#)] [[PubMed](#)]
206. Cole, B.J.; Pascual-Garrido, C.; Grumet, R.C. Surgical Management of Articular Cartilage Defects in the Knee. *JBJS* **2009**, *91*, 1778–1790.
207. Kreuz, P.C.; Steinwachs, M.R.; Erggelet, C.; Krause, S.J.; Konrad, G.; Uhl, M.; Südkamp, N. Results after Microfracture of Full-Thickness Chondral Defects in Different Compartments in the Knee. *Osteoarthr. Cartil.* **2006**, *14*, 1119–1125. [[CrossRef](#)]
208. Steadman, J.R.; Rodkey, W.G.; Rodrigo, J.J. Microfracture: Surgical Technique and Rehabilitation to Treat Chondral Defects. *Clin. Orthop. Relat. Res.* **2001**, *391*, S362–S369. [[CrossRef](#)] [[PubMed](#)]
209. Steadman, J.R.; Briggs, K.K.; Rodrigo, J.J.; Kocher, M.S.; Gill, T.J.; Rodkey, W.G. Outcomes of Microfracture for Traumatic Chondral Defects of the Knee: Average 11-Year Follow-Up. *Arthrosc. J. Arthrosc. Relat. Surg.* **2003**, *19*, 477–484. [[CrossRef](#)]
210. Frisbie, D.D.; Trotter, G.W.; Powers, B.E.; Rodkey, W.G.; Steadman, J.R.; Howard, R.D.; Park, R.D.; McIlwraith, C.W. Arthroscopic Subchondral Bone Plate Microfracture Technique Augments Healing of Large Chondral Defects in the Radial Carpal Bone and Medial Femoral Condyle of Horses. *Vet. Surg.* **1999**, *28*, 242–255. [[CrossRef](#)] [[PubMed](#)]
211. Asik, M.; Ciftci, F.; Sen, C.; Erdil, M.; Atalar, A. The Microfracture Technique for the Treatment of Full-Thickness Articular Cartilage Lesions of the Knee: Midterm Results. *Arthrosc. J. Arthrosc. Relat. Surg.* **2008**, *24*, 1214–1220. [[CrossRef](#)] [[PubMed](#)]
212. Steadman, J.R.; Rodkey, W.G.; Briggs, K.K. Microfracture: Its History and Experience of the Developing Surgeon. *Cartilage* **2010**, *1*, 78–86. [[CrossRef](#)]
213. Frisbie, D.D.; Oxford, J.T.; Southwood, L.; Trotter, G.W.; Rodkey, W.G.; Steadman, J.R.; Goodnight, J.L.; McIlwraith, C.W. Early Events in Cartilage Repair After Subchondral Bone Microfracture. *Clin. Orthop. Relat. Res.* **2003**, *407*, 215–227. [[CrossRef](#)]
214. Redondo, M.; Beer, A.; Yanke, A. Cartilage Restoration: Microfracture and Osteochondral Autograft Transplantation. *J. Knee Surg.* **2018**, *31*, 231–238. [[CrossRef](#)] [[PubMed](#)]
215. Tran-Khanh, N.; Hoemann, C.D.; McKee, M.D.; Henderson, J.E.; Buschmann, M.D. Aged Bovine Chondrocytes Display a Diminished Capacity to Produce a Collagen-Rich, Mechanically Functional Cartilage Extracellular Matrix. *J. Orthop. Res.* **2005**, *23*, 1354–1362. [[CrossRef](#)]
216. Welton, K.L.; Logterman, S.; Bartley, J.H.; Vidal, A.F.; McCarty, E.C. Knee Cartilage Repair and Restoration: Common Problems and Solutions. *Clin. Sports Med.* **2018**, *37*, 307–330. [[CrossRef](#)] [[PubMed](#)]
217. Furukawa, T.; Eyre, D.R.; Koide, S.; Glimcher, M.J. Biochemical Studies on Repair Cartilage Resurfacing Experimental Defects in the Rabbit Knee. *J. Bone Jt. Surg. Am.* **1980**, *62*, 79–89. [[CrossRef](#)]
218. Bae, D.K.; Yoon, K.H.; Song, S.J. Cartilage Healing After Microfracture in Osteoarthritic Knees. *Arthrosc. J. Arthrosc. Relat. Surg.* **2006**, *22*, 367–374. [[CrossRef](#)] [[PubMed](#)]
219. Gobbi, A.; Nunag, P.; Malinowski, K. Treatment of Full Thickness Chondral Lesions of the Knee with Microfracture in a Group of Athletes. *Knee Surg. Sports Traumatol. Arthrosc.* **2005**, *13*, 213–221. [[CrossRef](#)]
220. Franke, O.; Durst, K.; Maier, V.; Göken, M.; Birkholz, T.; Schneider, H.; Hennig, F.; Gelse, K. Mechanical Properties of Hyaline and Repair Cartilage Studied by Nanoindentation. *Acta Biomater.* **2007**, *3*, 873–881. [[CrossRef](#)]
221. Shapiro, F.; Koide, S.; Glimcher, M.J. Cell Origin and Differentiation in the Repair of Full-Thickness Defects of Articular Cartilage. *J. Bone Jt. Surg.* **1993**, *75*, 532–553. [[CrossRef](#)]
222. Sellers, R.S.; Peluso, D.; Morris, E.A. The Effect of Recombinant Human Bone Morphogenetic Protein-2 (rhBMP-2) on the Healing of Full-Thickness Defects of Articular Cartilage. *J. Bone Jt. Surg.* **1997**, *79*, 1452–1463. [[CrossRef](#)]
223. Ebenstein, D.M.; Kuo, A.; Rodrigo, J.J.; Reddi, A.H.; Ries, M.; Pruitt, L. A Nanoindentation Technique for Functional Evaluation of Cartilage Repair Tissue. *J. Mater. Res.* **2004**, *19*, 273–281. [[CrossRef](#)]
224. Lohmander, L.S. Articular Cartilage and Osteoarthritis. The Role of Molecular Markers to Monitor Breakdown, Repair and Disease. *J. Anat.* **1994**, *184 Pt 3*, 477. [[PubMed](#)]
225. Brown, W.E.; Potter, H.G.; Marx, R.G.; Wickiewicz, T.L.; Warren, R.F. Magnetic Resonance Imaging Appearance of Cartilage Repair in the Knee. *Clin. Orthop. Relat. Res.* **2004**, *422*, 214–223. [[CrossRef](#)] [[PubMed](#)]

226. Mithoefer, K.; Williams, R.J.; Warren, R.F.; Potter, H.G.; Spock, C.R.; Jones, E.C.; Wickiewicz, T.L.; Marx, R.G. The Microfracture Technique for the Treatment of Articular Cartilage Lesions in the Knee: A Prospective Cohort Study. *J. Bone Jt. Surg.* **2005**, *87*, 1911–1920. [[CrossRef](#)]
227. Mithoefer, K.; Williams, R.J.; Warren, R.F.; Potter, H.G.; Spock, C.R.; Jones, E.C.; Wickiewicz, T.L.; Marx, R.G. Chondral Resurfacing of Articular Cartilage Defects in the Knee with the Microfracture Technique: Surgical Technique. *J. Bone Jt. Surg.-Am. Vol.* **2006**, *88*, 294–304. [[CrossRef](#)]
228. Vanlauwe, J.; Saris, D.B.F.; Victor, J.; Almqvist, K.F.; Bellemans, J.; Luyten, F.P.; TIG/ACT/01/2000&EXT Study Group; Bohnsack, M.; Claes, T.; Fortems, Y.; et al. Five-Year Outcome of Characterized Chondrocyte Implantation Versus Microfracture for Symptomatic Cartilage Defects of the Knee: Early Treatment Matters. *Am. J. Sports Med.* **2011**, *39*, 2566–2574. [[CrossRef](#)] [[PubMed](#)]
229. Volz, M.; Schaumburger, J.; Frick, H.; Grifka, J.; Anders, S. A Randomized Controlled Trial Demonstrating Sustained Benefit of Autologous Matrix-Induced Chondrogenesis over Microfracture at Five Years. *Int. Orthop. (SICOT)* **2017**, *41*, 797–804. [[CrossRef](#)] [[PubMed](#)]
230. Orth, P.; Gao, L.; Madry, H. Microfracture for Cartilage Repair in the Knee: A Systematic Review of the Contemporary Literature. *Knee Surg. Sports Traumatol. Arthrosc.* **2020**, *28*, 670–706. [[CrossRef](#)] [[PubMed](#)]
231. Marmotti, A.; De Girolamo, L.; Bonasia, D.E.; Bruzzone, M.; Mattia, S.; Rossi, R.; Montaruli, A.; Dettoni, F.; Castoldi, F.; Peretti, G. Bone Marrow Derived Stem Cells in Joint and Bone Diseases: A Concise Review. *Int. Orthop. (SICOT)* **2014**, *38*, 1787–1801. [[CrossRef](#)]
232. Lee, Y.H.D.; Suzer, F.; Thermann, H. Autologous Matrix-Induced Chondrogenesis in the Knee: A Review. *Cartilage* **2014**, *5*, 145–153. [[CrossRef](#)]
233. Bartz, R.L.; Kamaric, E.; Noble, P.C.; Lintner, D.; Bocell, J. Topographic Matching of Selected Donor and Recipient Sites for Osteochondral Autografting of the Articular Surface of the Femoral Condyles. *Am. J. Sports Med.* **2001**, *29*, 207–212. [[CrossRef](#)]
234. Dekker, T.J.; Aman, Z.S.; DePhillipo, N.N.; Dickens, J.F.; Anz, A.W.; LaPrade, R.F. Chondral Lesions of the Knee: An Evidence-Based Approach. *J. Bone Jt. Surg.* **2021**, *103*, 629–645. [[CrossRef](#)]
235. Ahmad, C.S.; Cohen, Z.A.; Levine, W.N.; Ateshian, G.A.; Van, C.M. Biomechanical and Topographic Considerations for Autologous Osteochondral Grafting in the Knee. *Am. J. Sports Med.* **2001**, *29*, 201–206. [[CrossRef](#)] [[PubMed](#)]
236. Hangody, L.; Vásárhelyi, G.; Hangody, L.R.; Sükösd, Z.; Tibay, G.; Bartha, L.; Bodó, G. Autologous Osteochondral Grafting—Technique and Long-Term Results. *Injury* **2008**, *39*, 32–39. [[CrossRef](#)]
237. Hangody, L.; Füles, P. Autologous Osteochondral Mosaicplasty for the Treatment of Full-Thickness Defects of Weight-Bearing Joints: Ten Years of Experimental and Clinical Experience. *JBJS* **2003**, *85* (Suppl. S2), 25–32. [[CrossRef](#)]
238. Makino, T.; Fujioka, H.; Terukina, M.; Yoshiya, S.; Matsui, N.; Kurosaka, M. The Effect of Graft Sizing on Osteochondral Transplantation. *Arthrosc. J. Arthrosc. Relat. Surg.* **2004**, *20*, 837–840. [[CrossRef](#)]
239. Nakaji, N.; Fujioka, H.; Nagura, I.; Kokubu, T.; Makino, T.; Sakai, H.; Kuroda, R.; Doita, M.; Kurosaka, M. The Structural Properties of an Osteochondral Cylinder Graft-Recipient Construct on Autologous Osteochondral Transplantation. *Arthrosc. J. Arthrosc. Relat. Surg.* **2006**, *22*, 422–427. [[CrossRef](#)]
240. Kuroki, H.; Nakagawa, Y.; Mori, K.; Ikeuchi, K.; Nakamura, T. Mechanical Effects of Autogenous Osteochondral Surgical Grafting Procedures and Instrumentation on Grafts of Articular Cartilage. *Am. J. Sports Med.* **2004**, *32*, 612–620. [[CrossRef](#)]
241. Lane, J.G.; Tontz, W.L.; Ball, S.T.; Massie, J.B.; Chen, A.C.; Bae, W.C.; Amiel, M.E.; Sah, R.L.; Amiel, D. A Morphologic, Biochemical, and Biomechanical Assessment of Short-Term Effects of Osteochondral Autograft Plug Transfer in an Animal Model. *Arthrosc. J. Arthrosc. Relat. Surg.* **2001**, *17*, 856–863. [[CrossRef](#)] [[PubMed](#)]
242. Nam, E.K.; Makhsous, M.; Koh, J.; Bowen, M.; Nuber, G.; Zhang, L.-Q. Biomechanical and Histological Evaluation of Osteochondral Transplantation in a Rabbit Model. *Am. J. Sports Med.* **2004**, *32*, 308–316. [[CrossRef](#)]
243. O'Driscoll, S.W.; Keeley, F.W.; Salter, R.B. The Chondrogenic Potential of Free Autogenous Periosteal Grafts for Biological Resurfacing of Major Full-Thickness Defects in Joint Surfaces under the Influence of Continuous Passive Motion. An Experimental Investigation in the Rabbit. *J. Bone Jt. Surg. Am.* **1986**, *68*, 1017–1035. [[CrossRef](#)]
244. Camp, C.L.; Stuart, M.J.; Krych, A.J. Current Concepts of Articular Cartilage Restoration Techniques in the Knee. *Sports Health* **2014**, *6*, 265–273. [[CrossRef](#)]
245. Bexkens, R.; Ogink, P.T.; Doornberg, J.N.; Kerkhoffs, G.M.M.J.; Eygendaal, D.; Oh, L.S.; Van Den Bekerom, M.P.J. Donor-Site Morbidity after Osteochondral Autologous Transplantation for Osteochondritis Dissecans of the Capitellum: A Systematic Review and Meta-Analysis. *Knee Surg. Sports Traumatol. Arthrosc.* **2017**, *25*, 2237–2246. [[CrossRef](#)]
246. Andrade, R.; Nunes, J.; Hinckel, B.B.; Gruskay, J.; Vasta, S.; Bastos, R.; Oliveira, J.M.; Reis, R.L.; Gomoll, A.H.; Espregueira-Mendes, J. Cartilage Restoration of Patellofemoral Lesions: A Systematic Review. *Cartilage* **2021**, *13*, 575–735. [[CrossRef](#)]
247. Solheim, E.; Hegna, J.; Strand, T.; Harlem, T.; Inderhaug, E. Randomized Study of Long-Term (15–17 Years) Outcome After Microfracture Versus Mosaicplasty in Knee Articular Cartilage Defects. *Am. J. Sports Med.* **2018**, *46*, 826–831. [[CrossRef](#)] [[PubMed](#)]
248. Knutsen, G.; Drogset, J.O.; Engebretsen, L.; Grøntvedt, T.; Isaksen, V.; Ludvigsen, T.C.; Roberts, S.; Solheim, E.; Strand, T.; Johansen, O. A Randomized Trial Comparing Autologous Chondrocyte Implantation with Microfracture: Findings at Five Years. *J. Bone Jt. Surg.* **2007**, *89*, 2105–2112. [[CrossRef](#)]
249. Briggs, T.W.R.; Mahroof, S.; David, L.A.; Flannelly, J.; Pringle, J.; Bayliss, M. Histological Evaluation of Chondral Defects after Autologous Chondrocyte Implantation of the Knee. *J. Bone Jt. Surgery. Br. Vol.* **2003**, *85-B*, 1077–1083. [[CrossRef](#)]

250. Peterson, L.; Brittberg, M.; Kiviranta, I.; Åkerlund, E.L. Autologous Chondrocyte Transplantation. *Am. J. Sports Med.* **2002**, *30*, 2–12. [[CrossRef](#)]
251. Roberts, S.; McCall, I.W.; Darby, A.J.; Menage, J.; Evans, H.; Harrison, P.E.; Richardson, J.B. Autologous Chondrocyte Implantation for Cartilage Repair: Monitoring Its Success by Magnetic Resonance Imaging and Histology. *Arthritis Res. Ther.* **2003**, *5*, R60. [[CrossRef](#)]
252. Vasara, A.I.; Nieminen, M.T.; Jurvelin, J.S.; Peterson, L.; Lindahl, A.; Kiviranta, I. Indentation Stiffness of Repair Tissue after Autologous Chondrocyte Transplantation. *Clin. Orthop. Relat. Res.* **2005**, *433*, 233–242. [[CrossRef](#)]
253. Henderson, I.; Lavigne, P.; Valenzuela, H.; Oakes, B. Autologous Chondrocyte Implantation: Superior Biologic Properties of Hyaline Cartilage Repairs. *Clin. Orthop. Relat. Res.* **2007**, *455*, 253–261. [[CrossRef](#)]
254. Peterson, L.; Minas, T.; Brittberg, M.; Nilsson, A.; Sjögren-Jansson, E.; Lindahl, A. Two- to 9-Year Outcome After Autologous Chondrocyte Transplantation of the Knee. *Clin. Orthop. Relat. Res.* **2000**, *374*, 212–234. [[CrossRef](#)]
255. Nixon, A.J.; Rickey, E.; Butler, T.J.; Scimeca, M.S.; Moran, N.; Matthews, G.L. A Chondrocyte Infiltrated Collagen Type I/III Membrane (MACI[®] Implant) Improves Cartilage Healing in the Equine Patellofemoral Joint Model. *Osteoarthr. Cartil.* **2015**, *23*, 648–660. [[CrossRef](#)]
256. Jones, C.W.; Willers, C.; Keogh, A.; Smolinski, D.; Fick, D.; Yates, P.J.; Kirk, T.B.; Zheng, M.H. Matrix-Induced Autologous Chondrocyte Implantation in Sheep: Objective Assessments Including Confocal Arthroscopy. *J. Orthop. Res.* **2008**, *26*, 292–303. [[CrossRef](#)]
257. Willers, C.; Chen, J.; Wood, D.; Xu, J.; Zheng, M.H. Autologous Chondrocyte Implantation with Collagen Bioscaffold for the Treatment of Osteochondral Defects in Rabbits. *Tissue Eng.* **2005**, *11*, 1065–1076. [[CrossRef](#)]
258. Hinckel, B.B.; Gomoll, A.H. Autologous Chondrocytes and Next-Generation Matrix-Based Autologous Chondrocyte Implantation. *Clin. Sports Med.* **2017**, *36*, 525–548. [[CrossRef](#)]
259. Lee, C.R.; Grodzinsky, A.J.; Hsu, H.-P.; Martin, S.D.; Spector, M. Effects of Harvest and Selected Cartilage Repair Procedures on the Physical and Biochemical Properties of Articular Cartilage in the Canine Knee. *J. Orthop. Res.* **2000**, *18*, 790–799. [[CrossRef](#)]
260. Russlies, M.; Rütther, P.; Köller, W.; Stomberg, P.; Behrens, P. Biomechanical properties of cartilage repair tissue after different cartilage repair procedures in sheep. *Z. Orthop. Ihre Grenzgeb.* **2003**, *141*, 465–471. [[CrossRef](#)]
261. Griffin, D.J.; Bonnevie, E.D.; Lachowsky, D.J.; Hart, J.C.A.; Sparks, H.D.; Moran, N.; Matthews, G.; Nixon, A.J.; Cohen, I.; Bonassar, L.J. Mechanical Characterization of Matrix-Induced Autologous Chondrocyte Implantation (MACI[®]) Grafts in an Equine Model at 53 Weeks. *J. Biomech.* **2015**, *48*, 1944–1949. [[CrossRef](#)]
262. Schuette, H.B.; Kraeutler, M.J.; McCarty, E.C. Matrix-Assisted Autologous Chondrocyte Transplantation in the Knee: A Systematic Review of Mid- to Long-Term Clinical Outcomes. *Orthop. J. Sports Med.* **2017**, *5*, 232596711770925. [[CrossRef](#)]
263. Yang, J.; Zhang, Y.S.; Yue, K.; Khademhosseini, A. Cell-Laden Hydrogels for Osteochondral and Cartilage Tissue Engineering. *Acta Biomater.* **2017**, *57*, 1–25. [[CrossRef](#)]
264. Koh, Y.-G.; Lee, J.-A.; Kim, Y.S.; Lee, H.Y.; Kim, H.J.; Kang, K.-T. Optimal Mechanical Properties of a Scaffold for Cartilage Regeneration Using Finite Element Analysis. *J. Tissue Eng.* **2019**, *10*, 204173141983213. [[CrossRef](#)]
265. Rai, V.; Dilisio, M.F.; Dietz, N.E.; Agrawal, D.K. Recent Strategies in Cartilage Repair: A Systemic Review of the Scaffold Development and Tissue Engineering: TISSUE ENGINEERING, SCAFFOLD, AND CARTILAGE REPAIR. *J. Biomed. Mater. Res.* **2017**, *105*, 2343–2354. [[CrossRef](#)]
266. Grad, S.; Loparic, M.; Peter, R.; Stolz, M.; Aebi, U.; Alini, M. Sliding Motion Modulates Stiffness and Friction Coefficient at the Surface of Tissue Engineered Cartilage. *Osteoarthr. Cartil.* **2012**, *20*, 288–295. [[CrossRef](#)]
267. Tanaka, Y.; Yamaoka, H.; Nishizawa, S.; Nagata, S.; Ogasawara, T.; Asawa, Y.; Fujihara, Y.; Takato, T.; Hoshi, K. The Optimization of Porous Polymeric Scaffolds for Chondrocyte / Atelocollagen Based Tissue-Engineered Cartilage. *Biomaterials* **2010**, *31*, 4506–4516. [[CrossRef](#)]
268. Spiller, K.L.; Maher, S.A.; Lowman, A.M. Hydrogels for the Repair of Articular Cartilage Defects. *Tissue Eng. Part B Rev.* **2011**, *17*, 281–299. [[CrossRef](#)]
269. Elisseeff, J.; Puleo, C.; Yang, F.; Sharma, B. Advances in Skeletal Tissue Engineering with Hydrogels. *Orthod. Craniofac Res.* **2005**, *8*, 150–161. [[CrossRef](#)]
270. Wei, W.; Ma, Y.; Yao, X.; Zhou, W.; Wang, X.; Li, C.; Lin, J.; He, Q.; Leptihn, S.; Ouyang, H. Advanced Hydrogels for the Repair of Cartilage Defects and Regeneration. *Bioact. Mater.* **2021**, *6*, 998–1011. [[CrossRef](#)]
271. Wang, D.-A.; Varghese, S.; Sharma, B.; Strehin, I.; Fermanian, S.; Gorham, J.; Fairbrother, D.H.; Cascio, B.; Elisseeff, J.H. Multifunctional Chondroitin Sulphate for Cartilage Tissue–Biomaterial Integration. *Nat. Mater.* **2007**, *6*, 385–392. [[CrossRef](#)]
272. Abdel-Sayed, P.; Pioletti, D.P. Strategies for Improving the Repair of Focal Cartilage Defects. *Nanomedicine* **2015**, *10*, 2893–2905. [[CrossRef](#)]
273. Pattappa, G.; Schewior, R.; Hofmeister, I.; Seja, J.; Zellner, J.; Johnstone, B.; Docheva, D.; Angele, P. Physioxia Has a Beneficial Effect on Cartilage Matrix Production in Interleukin-1 Beta-Inhibited Mesenchymal Stem Cell Chondrogenesis. *Cells* **2019**, *8*, 936. [[CrossRef](#)]
274. Dennis, J.E.; Whitney, G.A.; Rai, J.; Fernandes, R.J.; Kean, T.J. Physioxia Stimulates Extracellular Matrix Deposition and Increases Mechanical Properties of Human Chondrocyte-Derived Tissue-Engineered Cartilage. *Front. Bioeng. Biotechnol.* **2020**, *8*, 590743. [[CrossRef](#)]

275. Pattappa, G.; Johnstone, B.; Zellner, J.; Docheva, D.; Angele, P. The Importance of Physioxia in Mesenchymal Stem Cell Chondrogenesis and the Mechanisms Controlling Its Response. *IJMS* **2019**, *20*, 484. [[CrossRef](#)]
276. Wang, D.W.; Fermor, B.; Gimble, J.M.; Awad, H.A.; Guilak, F. Influence of Oxygen on the Proliferation and Metabolism of Adipose Derived Adult Stem Cells. *J. Cell. Physiol.* **2005**, *204*, 184–191. [[CrossRef](#)] [[PubMed](#)]
277. Khan, W.S.; Adesida, A.B.; Hardingham, T.E. Hypoxic Conditions Increase Hypoxia-Inducible Transcription Factor 2 α and Enhance Chondrogenesis in Stem Cells from the Infrapatellar Fat Pad of Osteoarthritis Patients. *Arthritis Res. Ther.* **2007**, *9*, R55. [[CrossRef](#)]

Disclaimer/Publisher's Note: The statements, opinions and data contained in all publications are solely those of the individual author(s) and contributor(s) and not of MDPI and/or the editor(s). MDPI and/or the editor(s) disclaim responsibility for any injury to people or property resulting from any ideas, methods, instructions or products referred to in the content.